Check for updates

Enhancing postharvest quality of bananas: comparative study on the use ZnO and Ag$_2$O nanoparticles and ZnO/Ag$_2$O composites

Noluthando Noxolo Aruwajoye[1], Isaac Adeyemi Sanusi[2], Gabriel Sanjo Aruwajoye[3], Asanda Mditshwa[1] and Samson Zeray Tesfay[1]*

[1]Discipline of Horticultural Science, School of Agricultural, Earth and Environmental Sciences, University of KwaZulu-Natal, Pietermaritzburg, South Africa, [2]School of Life Sciences, University of KwaZulu-Natal, Pietermaritzburg, South Africa, [3]Focus Area for Human Metabolomics, North-West University, Potchefstroom, South Africa

The 'Cavendish' banana is cultivated for its flavor and nutritional value, but its climacteric nature leads to rapid ripening and reduced shelf life. Preserving postharvest quality is crucial for minimizing losses and ensuring consumer satisfaction. Nanoparticles such as ZnO and Ag$_2$O have shown promise in extending the shelf life and maintaining the quality of perishable fruits. Therefore, this study aimed to evaluate the efficacy of ZnO- and Ag$_2$O-enriched edible coatings on the postharvest physicochemical quality of 'Cavendish' bananas stored at ambient temperature. Bananas were treated with five different formulations: (1) moringa extract alone (MG), (2) moringa extract combined with carboxymethyl cellulose and glycerol (MG + CMC + GLY), (3) carboxymethyl cellulose and glycerol with Ag$_2$O nanoparticles (Ag$_2$O), (4) carboxymethyl cellulose and glycerol with ZnO nanoparticles (ZnO), and (5) carboxymethyl cellulose and glycerol with a combination of Ag$_2$O and ZnO nanoparticles (Ag$_2$O + ZnO). The effects on key quality parameters, including weight loss, color retention, total soluble solids, total acidity, pH, and peel structure, were assessed. At the end of the storage period, the fruits treated with ZnO + Ag$_2$O nanoparticles demonstrated a significantly lower decay incidence of 44.44% than the control (100%). Similarly, nanoparticle-enriched treatments maintained higher L* (1.46-fold), b*(1.38-fold), and h^o (1.11-fold) values than the control treatment. Remarkably, the Ag$_2$O + ZnO composite formulation showed the most significant positive effects on total acidity, pH, and stomatal cell integrity toward improving banana quality. This study highlights the potential of ZnO/Ag$_2$O composites as effective postharvest treatments to enhance banana quality and extend shelf life, providing a promising approach to reduce postharvest losses and ensure fruit quality during storage and transportation.

1 Introduction

'Cavendish' bananas are cultivated worldwide for their unique flavor and nutritional benefits. As a climacteric fruit, bananas undergo increased respiration rates and ethylene production as they ripen (Fukano and Tachiki, 2021; Al-Dairi et al., 2024). During ripening, various external and internal changes become apparent, including chlorophyll degradation, the production of volatiles such as phenylacetaldehyde and 3-methylbutanal, and alterations in the texture of the banana fruit (Kapoor et al., 2022; Pereira et al., 2021; Shi et al., 2022). These transformations are influenced by factors such as temperature, light, humidity, phytohormones, genes, and epigenetic factors (Matas et al., 2009; Li et al., 2021; Giovannoni et al., 2017; Li et al., 2022; Rahman et al., 2021). Consequently, the shelf life of the fruit diminishes, leading to a significant loss of fruit quality and eventual fruit and financial losses. To mitigate these rapid quality degradations, the implementation of effective postharvest preservation techniques is essential.

The postharvest perishability and marketability of fresh fruit pose a global challenge, significantly impacting the profitability of fruit farming (Singh et al., 2014). Postharvest losses for fruits and vegetables range from 28 to 55%, totaling approximately USD 750 billion each year (Karoney et al., 2024). These losses can be attributed to factors such as respiration, water loss, mechanical damage, microbial invasion, and rapid maturation, resulting in unfavorable sugar and acid ratios (Zhang et al., 2017). To mitigate these challenges, extensive research has focused on regulating the ripening process (Wilson et al., 2019; Belay et al., 2019; Ribeiro et al., 2021). Successful techniques include selecting cultivars less susceptible to rapid ripening and controlling gas atmospheres through modified atmosphere packaging and controlled atmosphere methods (Xiang et al., 2021; Ponce et al., 2021). The postharvest quality and shelf life of bananas can be significantly enhanced through various techniques tailored to the unique characteristics of the fruit. Nuamduang et al. (2024) studied modified atmosphere packaging. Polybutylene succinate pouches reduced moisture loss, maintained firmness, and delayed banana ripening. Controlled atmosphere storage also slows metabolic rates and reduces postharvest spoilage, increasing shelf life (Gularte et al., 2022). The choice of cultivar is also essential. 'Cavendish' banana cultivar has been widely grown commercially because it ripens more slowly than other cultivars. Hence, it is favored for extended storage and shipping in the commercial banana industry (Dale et al., 2017). Additional efforts such as edible coatings are being implemented to lower respiration, water loss, microbial invasion, and maturation toward extended shelf life (Paulo et al., 2021; Shinga and Fawole, 2023; Romero et al., 2022; Saleem et al., 2021; Malekshahi and ValizadehKaji, 2021; Vilaplana et al., 2020).

These coatings create a protective layer that influences the environment of the fruit (Dhall, 2013). This technique primarily helps by curbing the exchange of gases, which slows down the ripening process of the fruit and reduces spoilage (Dhall, 2013). The coatings also act as barriers against solutes, gases, and vapors, which are critical factors in preserving the overall quality of the produce (Yousuf et al., 2018). In edible coating formulations, various substances are incorporated to improve their effectiveness. These include agents designed to prevent microbial growth, modify texture, enhance flavors, and inhibit browning (Khalid et al., 2022).

Several studies have investigated the use of edible coatings to reduce postharvest losses and maintain quality in bananas. For instance, Maqbool et al. (2011) observed that chitosan coatings combined with gum arabic were effective (over 80% efficiency) in controlling anthracnose and extending the shelf life of bananas. Additionally, Dwivany et al. (2020) demonstrated that an edible carrageenan coating (1.5% inclusion; 20°C storage temperature) effectively extended the shelf life and quality of Cavendish bananas for an additional 6 days in comparison with the control, while 1.5% edible carrageenan inclusion, at room temperature, only extended the shelf life by 2 days. Similarly, Kim et al. (2022) found that carboxymethyl cellulose combined with *Morus alba* extracts effectively maintained banana quality and extended shelf life during storage over 15 days.

An emerging advancement in the use of edible coating is the integration of nanobiotechnology, which has great potential to enhance the performance of edible coatings by introducing novel materials and techniques for more effective postharvest preservation (Olunusi et al., 2024). Similarly, nanotechnologies have been employed in various industries, including the food and agri-food sectors, as well as in postharvest disease control (Chawla et al., 2021; Lang et al., 2021; Wahab et al., 2021: Sanusi et al., 2022). Nanomaterials, such as Fe_3O_4, TiO_2, Fe_2O_3, ZnO, Ag_2O, CoO, and carbon-based nanoparticles, exhibit desirable and remarkable properties including nanosized, high surface area to volume ratio, strong interfacial properties, catalytic potential, and antimicrobial (antibacterial and antifungal) properties. These attributes enhance their effectiveness in postharvest preservation of fruits such as bananas by delaying ripening, reducing spoilage, and maintaining fruit quality through improved pathogen inhibition. Studies on the effects of nanoparticle inclusion in non-toxic coating preservatives have shown their potential to maintain fruit quality postharvest. For example, Li et al. (2019) demonstrated that ZnO nanoparticle-incorporated active packaging (at 4°C for 12 days) effectively maintained the initial appearance quality, thereby preventing the browning index (1.33-fold) and desirable shelf life of 12 days for fresh-cut *Fuji* apples. Similarly, Ortiz-Duarte et al. (2019) found that silver nanoparticle-enriched coatings (at 5°C for 13 days) that significantly favor late softening of the melon (over 9 days) reduced microbial growth (after day 10) and maintained the quality of fresh-cut melon after day 13 compared to the control. However, the comparative efficacy of ZnO and Ag_2O nanoparticles and their composites, specifically for banana preservation, remains understudied, and in addition, there is still limited information about the effectiveness of these nanoparticles and their mode of action. Though the mechanism of cellular inhibition by nanoparticles is not well known, the inhibitory action of nanoparticles might be attributed to their ability to cause loss of DNA replication and halt the expression of ribosomal sub-unit proteins and enzymes essential for ATP production. It can also be suggested that the nanomaterials bind with cytoplasmic membranes through disruptive electrostatic interaction with potential for cellular destruction (Vizhi et al., 2016). This disruptive effect of nanoparticles is influenced by particle size, with smaller particles exhibiting a stronger inhibitory effect due to their increased interfacial area. This enhanced surface contact allows for greater impact overall (Araujo et al., 2012). Similarly, it can be alluded that nanomaterials produce reactive oxygen species (ROS) with toxic potential against the cell (Sanusi et al., 2019). Nanoparticles at high concentrations can also inhibit cellular through mechanisms such as

membrane disruption. Understanding the various activities of nanoparticles as constituents of preservative coating material makes it an attractive area of research. Moreover, there is a scarcity of information regarding the impact of metallic oxide nanoparticles as a constituent of fruit preservative coating formulation toward maintaining the original quality of the fruit postharvest. This can be of positive economic consequences helping avoid, reduce, or delay losses.

Therefore, this study aimed to evaluate the performance of coating formulations enriched with ZnO and Ag₂O as well as their combinations on the postharvest and physicochemical quality of 'Cavendish' banana fruit stored at ambient temperature.

2 Materials and methods

2.1 Fruit material

'Cavendish' bananas, characterized by their light green color with a faint yellow color (Figure 1), were procured from the Pietermaritzburg Fresh Produce Market in the Province of KwaZulu-Natal, South Africa (29.5418° S, 30.4077° E). The bananas were initially immersed in a 70% ethanol solution (v/v) for outer sterilization of the banana and allowed to air dry for ~10 min. Subsequently, the fruits were transported to the Postharvest Research Laboratory at the University of KwaZulu-Natal, South Africa. Fruits displaying bruising or disease were excluded from the study.

2.2 Chemical reagent

The catalogue of the main chemical reagents used for this study and their manufacturer specifications are listed below: $ZnSO_4.7H_2O$ (99.0% purity), $AgNO_3$ (99.2% purity), NaOH (97.0% purity), carboxymethyl cellulose (CMC), glycerol (99.0% purity), and distilled water. These chemicals (purchased from South Africa-based suppliers: Merck, Sigma-Aldrich) were of reagent grade and used without additional purification. The metallic oxide nanoparticles used in the current study are listed as follows: zinc oxide (99.9 weight% purity) and silver oxide (99.9 weight% purity).

2.3 Preparation of Ag₂O nanoparticle (Ag₂O NPs)

Twenty milliliters of $AgNO_3$ solution (0.02 M) was added to 1.5 M NaOH dropwise until the pH of the solution was 10. The mixture was subjected to microwave radiation (using a microwave oven, Samsung, Model: ME9114S1, South Africa) at 700 W for 30-s on, 60-s off for 4 min. The precipitates obtained were washed several times with distilled water. The grayish brown precipitates of Ag₂O NPs were dried in an oven at 70°C and then characterized using scanning electron microscope (SEM), transmission electron microscope (TEM), and Fourier infrared spectroscopy (FITR; Sanusi et al., 2019).
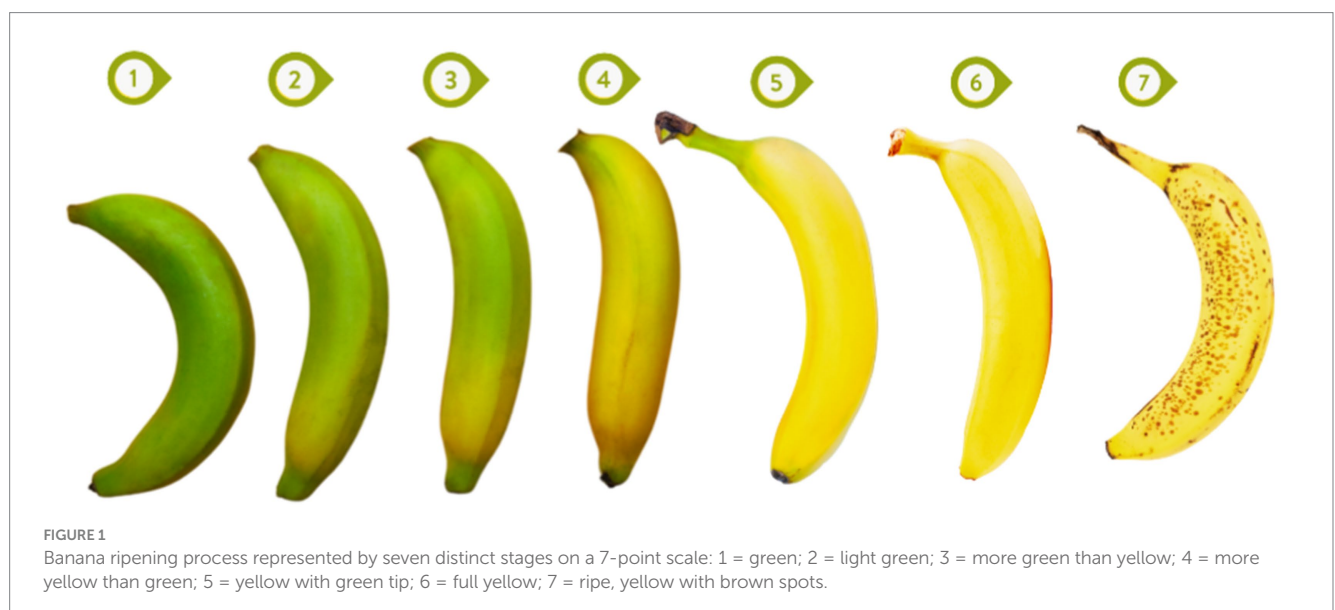
2.4 Preparation of ZnO nanoparticles (ZnO NPs)

$ZnSO_4.7H_2O$ (5.75 g) was dissolved in sterile distilled water after which 1 M NaOH solution was slowly added to adjust the solution to 11.29. The solution was placed in a microwave oven (Samsung, Model: ME9114S1, South Africa) for 3 min (700 W, 1-min on, 10-s off). The white precipitate was then rinsed with distilled water and dried at 70°C. Similarly, Scanning Electron Microscope (SEM), Transmission Electron Microscope (TEM) and Fourier Infrared Spectroscopy (FITR) were used for the characterization of the prepared ZnO NPs (Sanusi et al., 2019).

2.5 Characterization of nanoparticles

2.5.1 SEM characterization

The metallic composition microgram was obtained with scanning electron microscopy (SEM; ZEISS, Model ZEISS-EVO/LS15, UK).

FIGURE 1
Banana ripening process represented by seven distinct stages on a 7-point scale: 1 = green; 2 = light green; 3 = more green than yellow; 4 = more yellow than green; 5 = yellow with green tip; 6 = full yellow; 7 = ripe, yellow with brown spots.

Subsequent to the image and metallic composition analysis, the synthesized nanoparticle was gold-coated and mounted on an SEM grid coated with carbon. Afterward, using the SEM energy-dispersive X-ray spectroscopy (INCA x-stream-2, Oxford, UK), the metallic composition microgram was obtained.

2.5.2 TEM characterization

TEM microgram was obtained with a transmission electron microscope JEM-1400 (JEOL, USA). First, the nanoparticle was dispersed with a sonicator (DAWE Instrument, England) in an organic solvent for 15 min. The mixture using a hypothermal syringe was placed on a Formvar-coated copper grid and air dried for 15 min. The grid with the sample was mounted on a TEM grid holder and then inserted into the TEM for viewing and particle size annotation.

2.5.3 FTIR characterization

Fourier transform infrared (FTIR) analysis was obtained by FTIR spectroscopy using a Spectrum 100 (PerkinElmer, USA). Briefly, the synthesized nanoparticle sample was placed on the FTIR detector, and then the resultant spectrum was captured and recorded between 600 and 4,000 cm^{-1} wavelengths.

2.6 Preparation and application of edible coatings

2.6.1 Formulation

Hundred (100) grams of commercial *Moringa oleifera* leaves powder (10%; purchased from an agricultural farm in Newcastle, South Africa) was added to 1 L of water at 50°C, and the mixture was heated for 30 min. The mixture was then sieved using Whatman No. 1 filter paper. The obtained extract was included in all the formulations except the control formulation (Table 1). In four separate 100-ml beakers, 100 ml of moringa extract at 50°C was added to each beaker, followed by 1 g of CMC powder and continually mixed to achieve a CMC concentration of 1% (w/v). For the preparation of Ag$_2$O, ZnO, and Ag$_2$O + ZnO nanoparticle edible coatings, 0.5 g of Ag$_2$O was added to one beaker containing moringa extract and carboxymethyl cellulose (CMC), 0.5 g of ZnO was added to another beaker, and 0.25 g of Ag$_2$O and 0.25 g of ZnO were added to a third beaker. Five treatments were created (Table 1): (1) moringa extract alone (MG), (2) moringa extract combined with carboxymethyl cellulose and glycerol (MG + CMC + GLY), (3) carboxymethyl cellulose and glycerol with Ag$_2$O nanoparticles (Ag$_2$O), (4) carboxymethyl cellulose and glycerol with ZnO nanoparticles (ZnO), and (5) carboxymethyl cellulose and

glycerol with a combination of Ag$_2$O and ZnO nanoparticles (Ag$_2$O + ZnO). The treatment solutions were applied by dipping the fruit for 1 min, followed by air drying at room temperature on a laboratory bench for 45–60 min. The control was untreated. Each treatment consisted of three replicates, with each replicate containing three fruits per storage interval, totaling nine fruits per treatment for each storage interval. The bananas were kept at a temperature of 25°C for 12 days, and postharvest parameters were assessed every 3 days.

2.6.2 Fourier transform infrared analysis

The functional group modifications in MG, GLY, CMC, MG + GLY + CMC, ZnO NP, Ag$_2$O NP, and ZnO + Ag$_2$O NP were analyzed using Fourier transform infrared (FTIR) spectroscopy with a Spectrum 100 instrument from PerkinElmer, USA. The samples were placed on the FTIR detector, and the resulting spectra were recorded in transmittance mode across the wavenumber range of 500 to 4,000 cm^{-1}.

2.7 Fruit weight loss

For each treatment, three bananas per replicate were weighed individually at the beginning of the storage period using a RADWAG Electronic PS 4500. R2.M scale (Poland). The initial weight was recorded as Wi. The same bananas were weighed again at 3, 6, 9, and 12-day intervals. The cumulative weight loss was calculated as a percentage of the initial weight. The weight loss percentage was determined by the difference between the initial and final weights, using the formula in Equation 1:

$$\text{Weight Loss}\,(\%) = \frac{W_i - W_f}{Wi} \times 100 \tag{1}$$

where W_i represents the initial fruit weight and W_f represents the final fruit weight.

2.8 Decay incidence

Any banana showing black spots or noticeable signs of infection was considered diseased. This percentage was determined using the Equation 2 according to Hossain and Iqbal (2016):

$$\text{Decay incidence}\,(\%) = \frac{Number\ of\ infected\ banana}{Total\ of\ bananas} \times 100 \tag{2}$$

TABLE 1 Composition of edible coating treatments.

Treatment	Moringa extract (%)	Carboxymethyl cellulose (%)	Ag$_2$O (wt. %)	ZnO (wt. %)	Glycerol (mL)
Control	–	–	–	–	–
MG	10	–	–	–	5
MG + CMC + GLY	10	1	–	–	5
Ag$_2$O	10	1	0.5	–	5
ZnO	10	1	–	0.5	5
Ag$_2$O + ZnO	10	1	0.25	0.25	5

*5 ml of glycerol was added in every 100 as a plasticizer.

2.9 Color

Banana peel color measurements were conducted using a Konica Minolta Chroma Meter CR-400. For each sample, three measurements were averaged from three different positions on the peel. The device was calibrated with a white standard tile. The parameters measured were L* (lightness), a* (red/green), b* (yellow/blue), and h° (hue angle). The L* value ranges from 0 (black) to 100 (white); positive a* values indicate redness, whereas negative a* values indicate greenness; and positive b* values indicate yellowness, whereas negative b* values indicate blueness (Wall and Gentry, 2007; Becerril-Sánchez et al., 2021; Thewes et al., 2022).

2.10 Total soluble solids, pH, and titratable acids

Total soluble solids (TSS) were measured using a digital refractometer with a thermodynamic control system (RFM340 + Refractometer, Bellingham and Stanley Ltd., Basingstoke, Hants, UK). TSS was recorded as Brix, which is equivalent to TSS%. The method by Khaliq et al. (2019) was used to determine the titratable acidity (TA) of banana flesh. Briefly, 10 g of banana fruit without the peel was mixed with 40 ml of distilled water. A titration was then performed using a 0.1 mol L^{-1} NaOH solution until the banana juice caused the phenolphthalein indicator to turn pink, indicating the total acidity. TA was calculated using Equation 2, and results were expressed as a percentage of malic acid.

$$TA\left(\text{malic acid\%}\right) = \frac{0.067 \times 0.1\,\text{NaOH} \times \text{titter}\left(\text{ml}\right)}{\text{Juice}\left(\text{ml}\right)} \times 100 \qquad (3)$$

2.11 Scanning electron microscopy and energy-dispersive X-ray spectroscopy

The elements on the banana peels (untreated and coated samples) were analyzed using the energy-dispersive X-ray (EDX) via a scanning electron microscope (Model ZEISS-EVO/LS15, UK). The SEM–EDX was operated using an EDX detector (Oxford I, X-Max 80 mm^2), and the samples were sputter-coated with gold and mounted onto aluminum grids coated with carbon before being viewed at 55× magnification.

2.12 Statistical analysis

The collected data were subjected to analysis of variance (ANOVA) using GenStat statistical software (GenStat®, 20th edition, VSN International, Hemel Hempstead, UK). The least significant difference values (LSD; $p < 0.05$) were calculated for mean separation. Additionally, principal component analysis (PCA) and hierarchical clustering heat map (HCHM) were performed in order to gain comprehensive insight into the relationships between the different NP treatments and the variables (L, a, b, hue, weight loss, pH, TA, TSS). The PCA and HCHM were programmed using the pandas, Matplotlib, and numPy libraries of Python. For the HCHM, a hierarchical clustering algorithm was used to perform agglomerative clustering on the dataset, which produces a dendrogram. The dendrogram depicts the hierarchical relationships between the treatments and their variables based on their similarities. The length of the branches in the dendrogram is directly proportional to the extent of dissimilarity between clusters of variables, meaning the shorter the length, the higher the similarity. In addition, the numbers (graded 0–100) and color intensity of the HCHM represent the degree of correlation or similarity between pairs of variables (Nde et al., 2024).

3 Results and discussion

3.1 Characterization of the synthesized ZnO and Ag₂O nanoparticles

The metallic and oxygen unit as well as their percentage was obtained with the SEM-EDS, while the existence of the metallic oxide was confirmed by a strong signal of the metal and the oxygen unit (Figures 2, 3). Other elements in minute concentration were also observed. These elements include carbon, sulfur, silicon, and aluminum, and their presence was from residue precursor in the nanoparticle preparation, while the carbon presence was mainly due to the grid used in SEM analysis (carbon-coated grid). The transmission electron microscopy (TEM) images showed the shape of ZnO (irregular) and Ag₂O (spherical) nanoparticles and weak agglomeration (Figures 2, 3). Particle size range of 10–99 nm and 15–29 nm were recorded for ZnO and Ag₂O nanoparticles, respectively. The spectra of the ZnO and Ag₂O nanoparticles were below the wavelength of 1,000 nm (Figures 2, 3), which are characteristic of oxides of metallic nanoparticles and can be attributed to their inter-atomic vibrations. Other function peaks on the spectra indicated the stretching vibrations of –CH₃, -CH₂, =C-H, –C-H, C=O, -OH, and NH groups ascribed to absorbed atmospheric moisture, CO₂, and precursor residue (Kumar et al., 2013). Both nanoparticles were in varying sizes within the nano-range, with ZnO nanoparticles having a wider size range distribution. Usually, shape and size of nanoparticles as well as the surface charge are important properties that conferred nanoparticles their chemical stability, reactivity, catalytic properties, interaction, and specificity. Literature has shown that there is a strong correlation between nanoparticle biochemical activities and their catalytic functions (Sanusi et al., 2019). In the present study, the coat formulated with nanoparticle inclusion preserved the appearance of the bananas, delayed decay incidence, stable coloration, and stomata integrity. Additionally, nanomaterials in fruit coating formulations can enhance the mechanical properties of the biopolymer and water vapor resistance of fruit such as the banana fruit in this study. This can be attributed to the potential of nanomaterial to interact with fruit surface forming complex bonds by electrostatic force to serve as a gas barrier of the coating, thereby suppressing the respiration and water loss processes toward better preservative effect under favorable storage conditions (Meindrawan et al., 2018). For instance, in a study by Joshy et al. (2020), ZnO nanoparticle-based xanthan gum applied to apple and tomato fruit delayed the deterioration of apple and the tomatoes as well as reduced water loss. Similarly, Chandirika et al. (2018) reported on the effect of
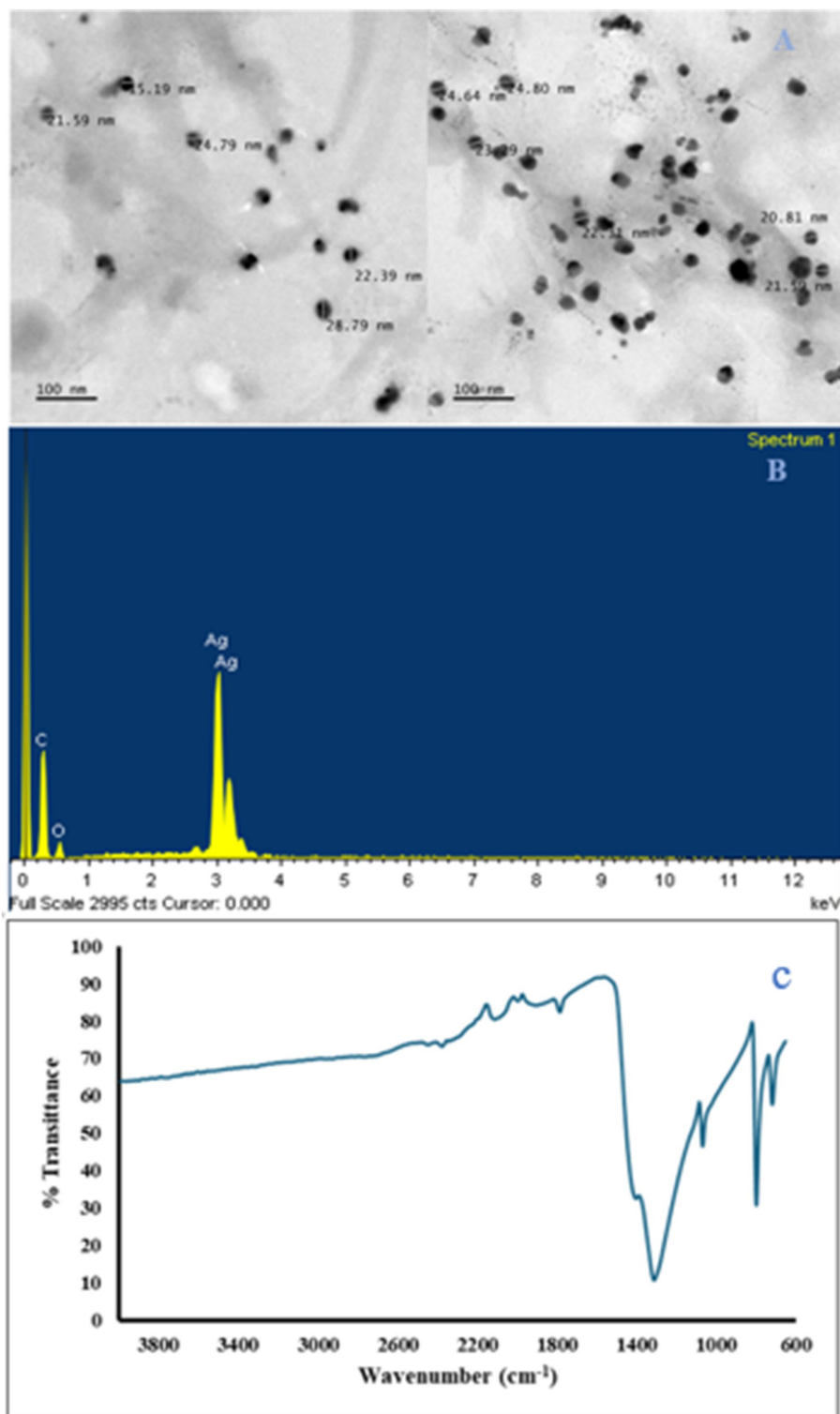
FIGURE 2
TEM images showing the Ag$_2$O particle size annotated (A), SEM−EDX microgram showing the elemental composition of metallic oxide (B), and FTIR spectrum for the Ag$_2$O nanoparticle (C).

the silver nanoparticles to improve the fruit quality metric of tomatoes at room temperature resulting in an extended shelf life from 16 to 21 days when compared with the control. Further analyses will be required to understand the mode of action of these nanoparticles to achieve the recorded outcomes.

3.2 Fourier transform infrared analysis of the formulations

The FTIR spectra (Figure 4) show different absorption peaks that correspond to the detectable functional groups and components
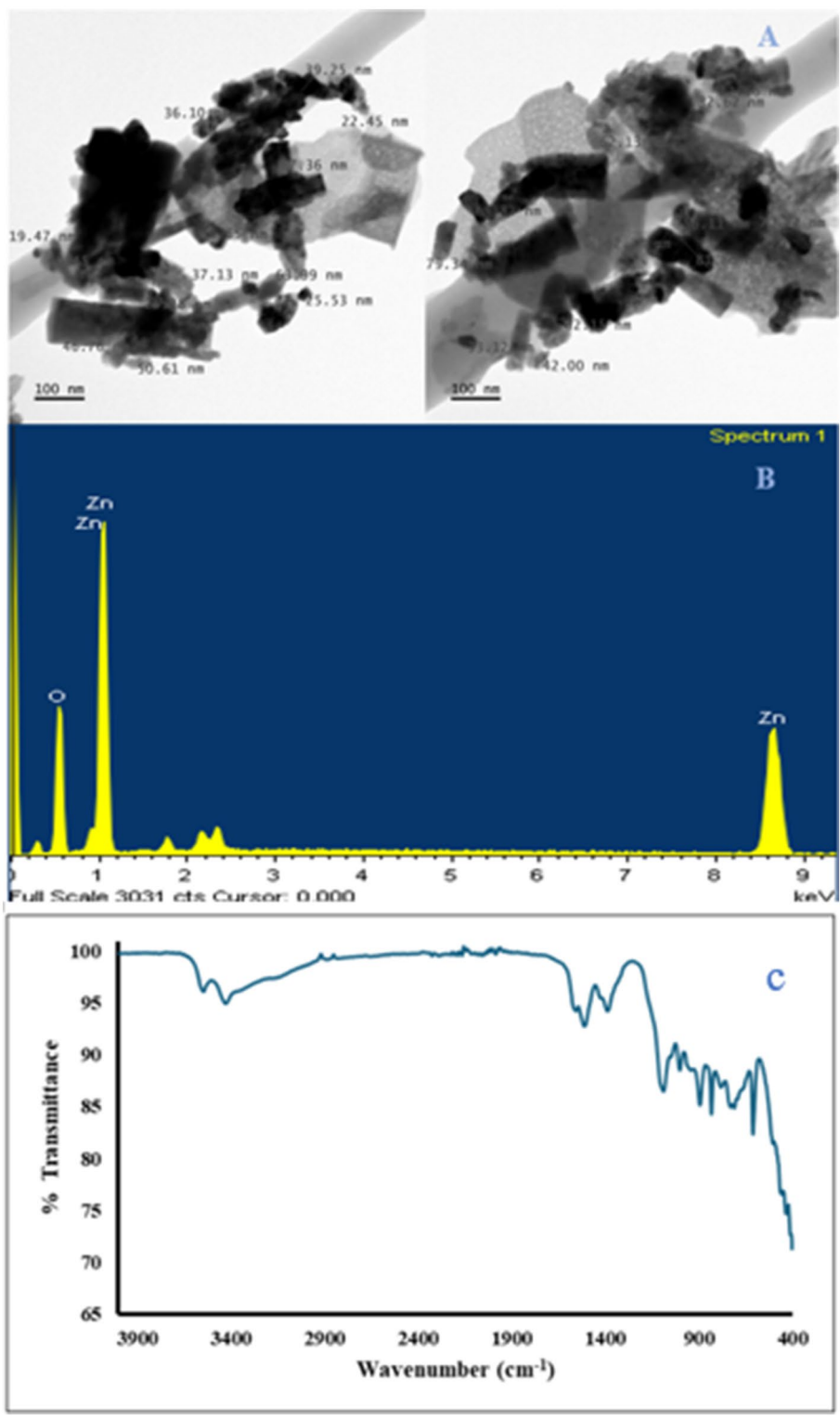
FIGURE 3
TEM images showing the ZnO particle size annotated **(A)**, SEM−EDX microgram showing the elemental composition of metallic oxide **(B)**, and FTIR spectrum for the ZnO nanoparticle **(C)**.

present in the formulated coat. Similar spectrum shapes were observed for all the formulated coats and were indicated by the similarity in the variations in the banding patterns observed with the glycerol spectrum uniquely different. Furthermore, the strong absorptive peaks associated with the glycerol at 2884 cm^{-1}, 2,943 cm^{-1}, and between 556 and 1,415 cm^{-1} compared to the formulations. In addition, coat formulation (MG + GLY + CMC) with glycerol had a sharp absorptive peak at 1061 cm^{-1}. This is an indication of the effect of glycerol as a
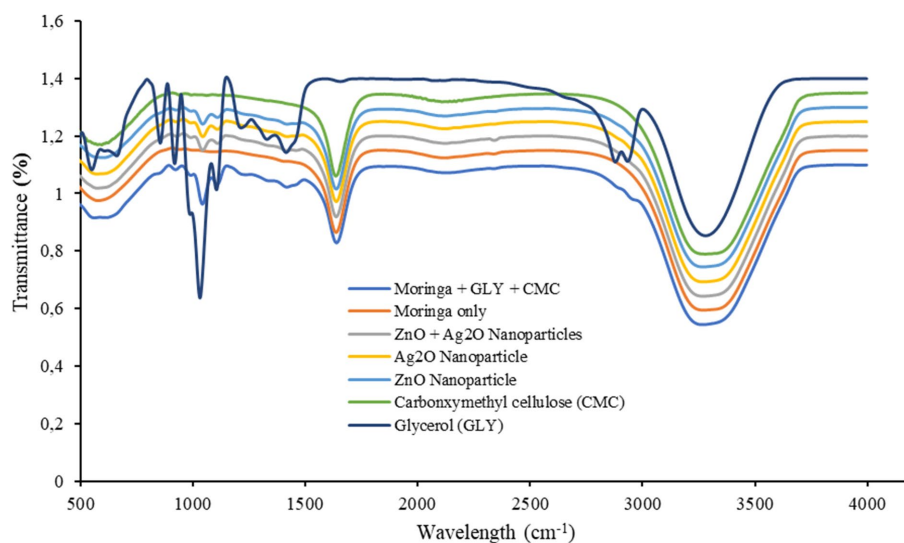
FIGURE 4
Fourier transform infrared (FTIR) spectroscopy of moringa + GLY + CMC, moringa only, ZnO + Ag$_2$O nanoparticles, Ag$_2$O nanoparticles, ZnO nanoparticles, carboxymethyl cellulose (CMC), and glycerol coat formulations.

constituent of the formulation corresponding to the preservative effect obtained with these glycerol-based formulations. The other similar peaks observed can be attributed to functional units with different indicative stretching peaks of –CH$_3$, -CH$_2$, =C-H, –C-H, C=O, -OH, and NH groups. These stretching peaks at 606, 1050, 1,644, and 3,306 cm^{-1} at various points on each formulation spectrum might be ascribed to absorbed moisture, CO$_2$, and residual precursor (Sanusi et al., 2019). Studies have reported that peak above 1,000 cm^{-1} might be related to stretching peaks of –CH$_3$, -CH$_2$, =C-H, and –C-H (Kumar et al., 2013). Moreover, the aromatic ring and ester units in the formulations are represented by C=O and C=C stretching peaks >1,000 cm^{-1} (Sanusi et al., 2022). In addition, the vibrations of C-O-C and C-O are related to the asymmetric stretching of carbohydrate presence in the formulations. Furthermore, a high peak >3,000 cm^{-1} can be linked to C-H and -OH vibrations of the intramolecular hydrogen within formulated components. The primary properties on which the different preservative effects observed with the different formulations in the current study could be ascribed to the presence of these groups and the inherent nature of formulations (Sanusi et al., 2022).

3.3 Effect of the formulation on the banana fruit

Various parameters, such as weight loss, pH, firmness, titratable acidity, total soluble solids, color stability, antioxidant activity, and disease incidence, have been used to assess the quality, integrity, and shelf life of fruits (Hudina et al., 2012). The effect of the formulations on the banana agreed with the results obtained from edible coatings (Dwivany et al., 2020). Remarkable weight loss reduction, color stability, desirable titratable acidity, and total soluble solids as well as longer shelf life were obtained with the formulations compared to bananas coated with the control formulation (Figures 5–7 and Table 2). This might be due to the thickness formulation, constituent

of the formulations, and storage temperature. A thick formulation and composition could have altered gas diffusion as well as water loss (Park et al., 1993) which could result in the generation of heat and anaerobic condition, leading to the fruit undergoing fermentation (ethanol production; Ke and Kader, 1989). Compared to other studies, the results revealed that lower temperatures could delay banana ripening than room temperature used in this study. This can probably be attributed in part to ethylene biosynthesis, which could be affected by temperature. An increase in storage temperature will increase ethylene biosynthesis, ripening processes, and metabolic processes consequently increasing banana ripening (Atta-Aly, 1992). Storage of fruits at lower temperatures could reduce the rate of respiration and transpiration of matured fruit, thereby preserving the water content of the fruit, while water loss could affect fruit quality (Dwivany et al., 2020). Based on the effect of formulation in peel color, weight loss, titratable acidity, and total soluble solids with storage at room temperature (25°C), the formulation could maintain shelf life longer than the control, showing the potential of the formulations to optimally delay banana ripening and physical quality as well as a taste of the banana fruit. As alterations during banana ripening are associated with (a) an increase in osmotic potential in the pulp due to the high conversion of starch into simple sugar, (b) loss in turgor pressure in the banana peel cells, and (c) water loss from the banana peel, the formulations, especially formulation with ZnO and Ag$_2$O nanoparticles, modulate these processes toward enhanced banana quality and shelf life.

3.3.1 Weight loss and decay incidence

The impact of nanoparticle-enriched edible coating on banana during storage was evaluated (Figure 5). Storage had a significant effect on weight loss ($p < 0.001$), while treatment alone ($p < 0.111$) and the interaction between treatment and storage time ($p = 0.89$) did not show significant effects. By the end of the storage period, weight loss values for the control (17.95%) and the various treatments (MG, MG + CMC + GLY, Ag$_2$O, ZnO, and the Ag$_2$O + ZnO composite)
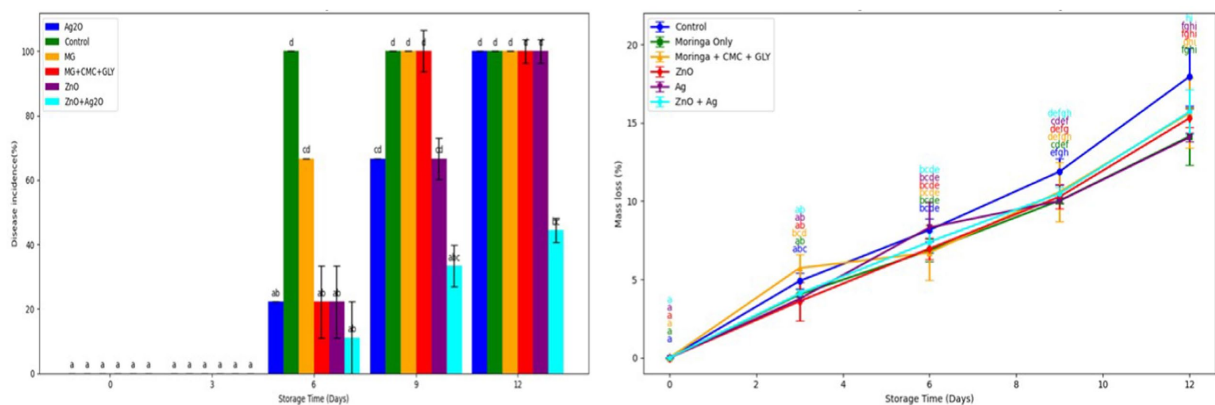
FIGURE 5
Effect of nanoparticle-enriched edible coating on weight loss during storage. Vertical bars represent the standard errors of the means.
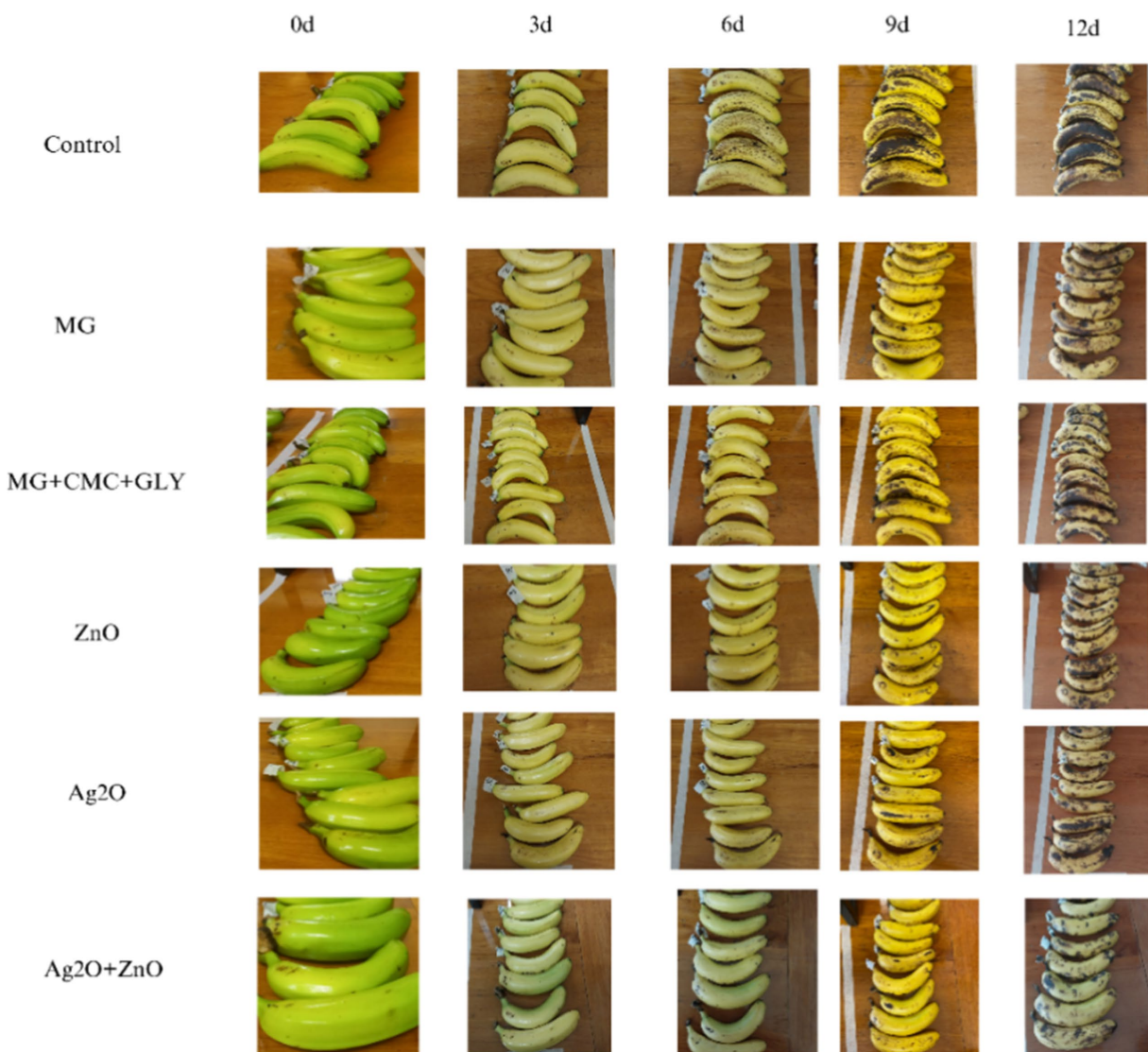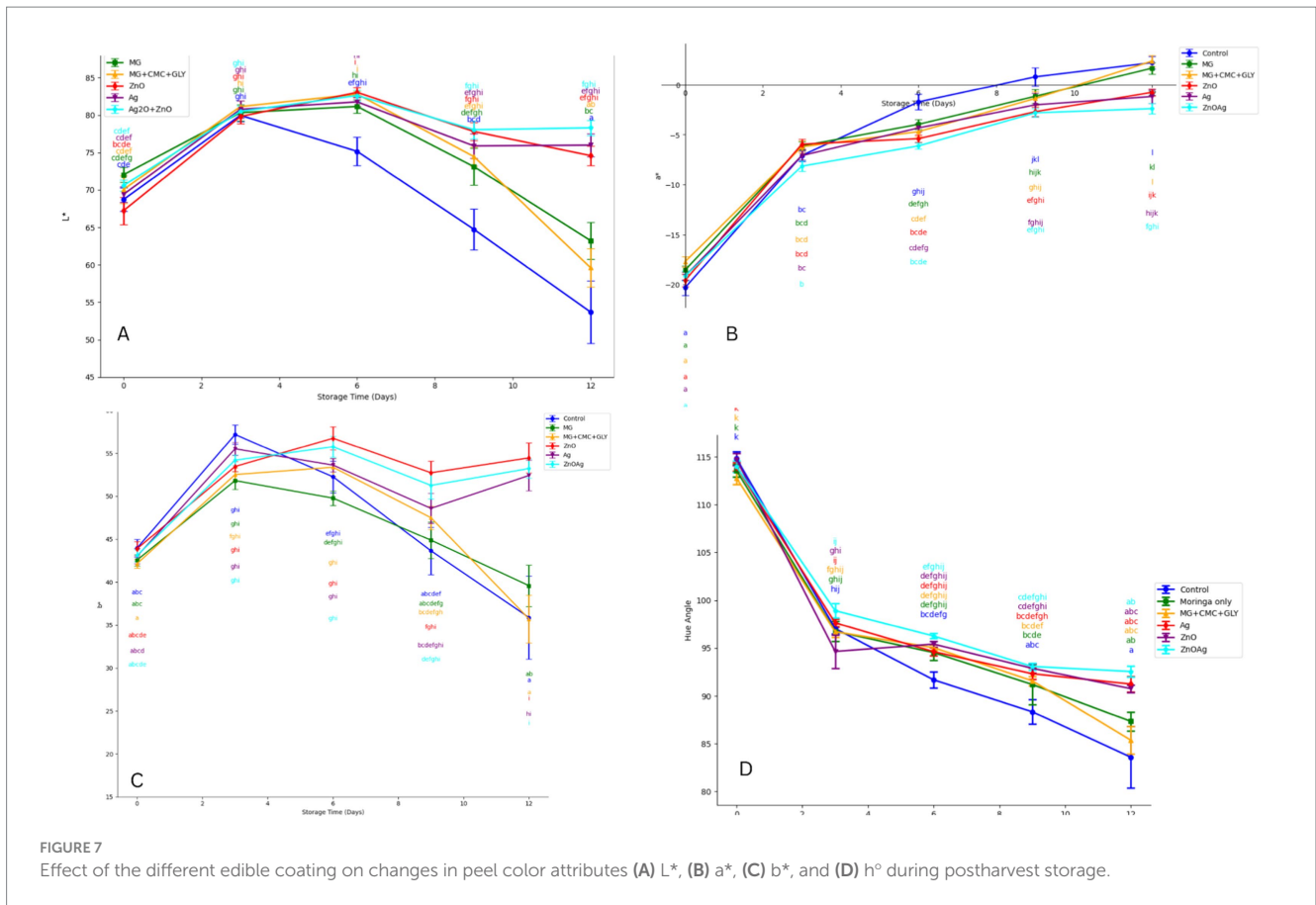

FIGURE 6
Changes in the physical appearance of bananas due to MG, MG + GLY + CMC, ZnO NP, Ag$_2$O NP, and ZnO + Ag$_2$O NP over a 12-day period at 25°C.

FIGURE 7
Effect of the different edible coating on changes in peel color attributes **(A)** L*, **(B)** a*, **(C)** b*, and **(D)** h° during postharvest storage.

ranged from 14.07 to 17.95%, with no significant differences observed between them. Weight loss is among the key physical quality indicators that show textural changes in fruits during postharvest storage due to rapid moisture losses that cause fruit shelving (Hasan et al., 2021). Variations in the formulation also resulted in a disparity in weight loss of the banana fruit. The presence of nanoparticles in the formulation resulted in lower banana fruit weight loss. The formulation most probably functions as a barrier to rapid transpiration or water vapor loss for the banana fruit (Baldwin et al., 1991). This can be attributed to the synergistic effect of nanoparticles, CMC, moringa, and the glycerol producing thick and multi-functional formulation on the banana peel. Moreover, these formulations could become a barrier to reducing the O_2 supply to the banana fruit, therefore modulating ripening toward longer shelf life (Maqbool et al., 2011). Hence previous report has shown that the presence of high levels of CO_2 and low levels of O_2 might inhibit the degradation of important pigments such as chlorophyll in the banana peel as well as ethylene release consequently, prolonging the banana ripening (Sorrentino et al., 2007). The effectiveness of using different coating formulations has been reported by numerous studies (Soradech et al., 2017; Dwivany et al., 2020). For instance, Soradech et al. (2017), investigated the combined impact of shellac and gelatin coatings on banana ripening, the authors observed mixture ratio of 3:2 of shellac and gelatin acted as a necessary physical barrier on the fruit that reduced weight loss and softening. This resulted in maintaining the integrity of the fruit over 30 days in comparison with the uncoated banana. Moreover, nanoparticles in coating formulations can enhance the mechanical properties of the biopolymer and water vapor resistance of the banana peel. For example,

Meindrawan et al. (2018) reported that the inclusion of zinc nanoparticles in carrageenan coating formulation reduced weight loss and total acidity, delay brownness, and decay of mango fruit compared with control without nanoparticles. This can be attributed to the potential of zinc to serve as a gas barrier of the coating, thereby suppressing the respiration and transpiration process toward a better preservative effect at room temperature storage as compared to carboxy methylcellulose alone, which has hydrophilic capability.

The effect of treatment, storage time, and interaction between treatment and storage time on decay incidents was significant ($p < 0.001$). Decay incidence increased progressively throughout the storage period, with the control exhibiting the most rapid progression, rising from 0% on days 0 and 3 to 100% by day 6. By day 9, all other treatments, except those involving nanoparticles (Ag_2O-66.67%, ZnO-66.67, and ZnO + Ag_2O-33.33%), had reached 100% decay incidence. At the end of the storage period, the fruits treated with ZnO + Ag_2O nanoparticles demonstrated a significantly lower decay incidence of 44.44%. The inclusion of metallic nanoparticles such as ZnO and Ag2O in the present study to fruit coatings has been known to provide additional antimicrobial and preservative effects on fruit surfaces even at low concentrations (<0.5%; Severino et al., 2014; Esparza-González et al., 2016; Acevedo-Fani et al., 2017). This is in agreement with a previous study, Gad and Zagzog (2017) showed that if xanthan gum and chitosan nanoparticles are mixed in a ratio of 1:2 compared to the uncoated and xanthan alone on guava fruit, Xanthan gum with chitosan nanoparticles decreased decay incidence, color change, maintained fruit firmness, and improved guava quality (vitamin C, good taste, and shelf life) compared with xanthan gum.

Treatment	Day	pH	TA (malic acid %)	TSS (%)
Control	0	4.88 ± 0.03[a]	0.29 ± 0.02[a]	2.86 ± 0.12[a]
	3	5.40 ± 0.01[b]	0.35 ± 0.01[abc]	6.00 ± 0.32[bcdefg]
	6	5.31 ± 0.01[b]	0.53 ± 0.02[h]	6.13 ± 0.11[cdefgh]
	9	5.92 ± 0.03[cd]	0.42 ± 0.02[def]	5.92 ± 0.03[bcdef]
	12	6.60 ± 0.01[gh]	0.39 ± 0.01[cdef]	5.29 ± 0.19[bc]
Moringa only	0	4.88 ± 0.03[a]	0.29 ± 0.02[a]	2.86 ± 0.12[a]
	3	5.39 ± 0.03[b]	0.36 ± 0.01[abcd]	5.59 ± 0.28[bcdef]
	6	5.42 ± 0.02[b]	0.51 ± 0.01[gh]	7.00 ± 0.24[ghij]
	9	6.03 ± 0.04[cde]	0.37 ± 0.01[bcd]	5.58 ± 0.23[bcdef]
	12	5.92 ± 0.02[cd]	0.39 ± 0.01[cdef]	4.97 ± 0.28[b]
MG + CMC + GLY	0	4.88 ± 0.03[a]	0.29 ± 0.02[a]	2.86 ± 0.12[a]
	3	5.31 ± 0.02[b]	0.32 ± 0.01[ab]	5.50 ± 0.15[bcdef]
	6	5.36 ± 0.02[b]	0.34 ± 0.01[abc]	7.36 ± 0.14[ij]
	9	6.19 ± 0.04[ef]	0.35 ± 0.01[abc]	5.47 ± 0.17[bcdef]
	12	6.38 ± 0.07[fg]	0.38 ± 0.01[bcde]	5.15 ± 0.16[bc]
Ag	0	4.88 ± 0.03[a]	0.29 ± 0.02[a]	2.86 ± 0.12[a]
	3	5.23 ± 0.01[b]	0.36 ± 0.00[abcd]	5.33 ± 0.07[bcd]
	6	5.27 ± 0.02[b]	0.38 ± 0.01[bcde]	6.46 ± 0.12[efghij]
	9	5.96 ± 0.02[cd]	0.41 ± 0.01[cdef]	6.12 ± 0.26[cdefgh]
	12	5.82 ± 0.04[c]	0.45 ± 0.01[fg]	6.48 ± 0.29[efghij]
ZnO	0	4.88 ± 0.03[a]	0.29 ± 0.02[a]	2.86 ± 0.12[a]
	3	5.36 ± 0.04[b]	0.36 ± 0.00[abcd]	6.34 ± 0.14[defghi]
	6	5.82 ± 0.16[c]	0.45 ± 0.01[fg]	7.39 ± 0.19[j]
	9	6.11 ± 0.04[de]	0.35 ± 0.01[abc]	6.50 ± 0.21[fghij]
	12	5.85 ± 0.01[c]	0.35 ± 0.00[abcd]	5.85 ± 0.01[bcdef]
ZnOAg	0	4.88 ± 0.03[a]	0.29 ± 0.02[a]	2.86 ± 0.12[a]
	3	6.47 ± 0.01[g]	0.36 ± 0.00[abcd]	5.68 ± 0.25[bcdef]
	6	5.40 ± 0.04[b]	0.39 ± 0.02[cde]	7.06 ± 0.11[hij]
	9	6.02 ± 0.04[cde]	0.35 ± 0.00[abcd]	7.28 ± 0.28[ij]
	12	6.75 ± 0.06[h]	0.44 ± 0.02[ef]	5.45 ± 0.15[bcde]

Letters as superscripts represent significant differences down the column [difference between treatments and storage days ($p > 0.001$)]. Data are presented as mean ± S.E.

3.3.2 Color of the banana peel

Color is a key visual attribute in assessing the quality and ripeness of fruits, as it often reflects underlying biochemical changes and influences consumer perception. The effects of treatment, storage time, and interaction between treatment and storage time on all color attributes were significant ($p < 0.001$). In Figure 7A, the L* values increased from day 0 to day 6 for all treatments followed by a gradual decline, except for the control with a sharp reduction in L* value after day 3. The results (Figure 7) show that the treatments had a significant effect on the L* value of the banana peel ($p < 0.001$). In contrast, the control showed a significant decrease in L* values after day 3 due to the appearance of black spots and brown pigmentation on the peel, indicative of faster ripening and browning. By the end of storage, all nanoparticle-enriched treatments exhibited the highest L* values

(ZnO: 74.59; Ag2O: 75.99; ZnOAg2O: 78.30), whereas the control had the lowest (53.68). As L* indicates the lightness of the fruit; lighter fruits have higher values, and as the fruit darkens, the L* value also decreases (Coimbra et al., 2023). Therefore, nanoparticles effectively maintained the lightness of the banana compared to other treatments by slowing down the ripening and browning of the banana fruit. Delayed ripening is usually a decrease in the rate of starch to simple sugars, whereas delayed browning can be attributed to slowing down or inhibition of the degradation of important pigment such as chlorophyll (Sorrentino et al., 2007).

In Figure 7B, the a* value in colorimetry is specifically designed to quantify the degree of change between the redness and greenness of the color of fruit (Sruthi et al., 2021). Positive a* values indicate a shift toward red, whereas negative values indicate a shift toward green. The a* value of the banana peel was significantly influenced by both the treatment and the interaction between treatment and storage ($p < 0.001$). On day 6, the control and MG treatments exhibited the highest a* values, at −1.72 and − 3.96, respectively, than all other treatments. At the end of storage, the control, MG, and MG + GLY + CMC had significantly higher a* values than the nano-enriched treatments (2.22, 1.67, and 2.38, respectively). The a* values for all NP-enriched treatments remained negative throughout storage (ZnO: −0.76; Ag2O: −1.18; ZnOAg2O: −2.39), indicating a consistent tendency toward greenness. This suggests that the nanoparticle-enriched treatments modulated the banana ripening metabolic processes in such a way that might have contributed to maintaining the greenish hue of the fruit peel during storage. Hence, the nanoparticle-enriched treatments have the desirable potential toward improving the marketability of the banana fruit.

Moreover, in Figure 7C, the b* value indicates the color change from blue to yellow (Zhou et al., 2022). Treatments with higher b* values show that the peel is more yellow. In particular, at the end of the storage all nanoparticle-enriched treatments (ZnO: 54.46, Ag2O: 52.42, and ZnOAg2O: 53.22) maintained the highest b* values, suggesting that nanoparticles effectively preserved the yellow coloration in the bananas than other treatments. Again, an indication of the nanoparticle-enriched formulations modulating the respiration, transpiration, ethylene production, chlorophyll degradation, and carotenoid synthesis processes to favor the preservation of the yellow coloration in the banana peel (Al-Dairi and Pathare, 2024). Conversely, a decrease in the b* value implies a reduction in yellow color intensity. The control, MG, and MG + GLY + CMC treatments exhibited the lowest b* values, measured at 38.55, 39.55, and 35.71, respectively. Banana peel color change from green to yellow to brown during storage has been attributed to chlorophyll degradation and carotenoid synthesis, which is responsible for the yellow color (Al-Dairi and Pathare, 2024).

The hº value decreased over time (Figure 7D), suggesting a change in the color hue of the fruit peel during storage. At the end of storage, all nanoparticle-enriched treatments had the highest hº values (ZnO: 90.75, Ag2O: 91.23, ZnOAg2O: 92.54), followed by the control, MG, and MG + GLY + CMC, which had values of 83.57, 87.32, and 85.32, respectively. The potential mechanisms of the nanoparticle-enriched formulations to achieve this effect have been elucidated above. This is in line with the report of previous studies where nanoparticle-enhanced coating formulations have been implemented in postharvest shelf life and quality of fruits. The nanomaterials were effective in enhancing color quality and fruit firmness, increasing antimicrobial

properties of formulations, regulating enzymatic activity, and lowering weight loss of fruits through the control of the transpiration process. Further underscoring the potential of nanoparticles improves the shelf life and the marketability of the banana fruit.

As banana ripens, chlorophyll which is responsible for the greenish color is broken down primarily by enzymes such as chlorophyllase and magnesium-dechelatase. Chlorophyllase removes a side chain from chlorophyll to form chlorophyllide. Magnesium dechelatase and pheophytinase further degrade chlorophyll, breaking it down into pheophorbide and pheophytin, leading to the loss of green color (Shinga and Fawole, 2023). Concurrently, as the chlorophyll is broken down, carotenoids are formed via the conversion of dimethylallyl pyrophosphate into phytoene, which is then desaturated to lycopene and cyclized to produce α-carotene, β-carotene, and xanthophylls (Maoka, 2020). This synthesis may be influenced by various factors, including ethylene production, temperature, and the presence of nanoparticles in the treatments applied to the bananas. Therefore, research efforts have focused on optimizing delaying color change, as it is a crucial indicator of ripeness and directly impacts marketability, consumer preference, and postharvest quality management (Othman et al., 2021; Geng et al., 2024; Odetayo et al., 2022).

3.3.3 pH, titratable acidity, and total soluble solids

The pH values in all treatments exhibited a general increase in pH during storage, with significant interactions between treatment and storage time ($p < 0.001$). Increase in the pH of the treatments could be ascribed to the increasing presence of hydrogen (H^+) in the banana pulp, resulting from the high concentration of acidic metabolites as it ripens (Mubarok et al., 2022). By the end of the storage period, the pH levels in the ZnO, Ag, and MG treatments were significantly lower than those in the control, ZnO + Ag, and MG + CMC + GLY treatments (Table 2). Usually, there is a close relationship between pH, TA, basic, and acidic metabolites. High acidic metabolite concentration lowers pH (<7), whereas low concentration of acidic metabolites results in higher pH values (>7). pH has an influenceable relationship with metabolic processes in this case ripening of the banana processes. Increasing acidity or alkalinity to extreme values could inhibit or halt metabolic processes (Sanusi et al., 2020).

In terms of titratable acidity (TA), the ZnO and ZnO + Ag treatments maintained higher values (0.2367 and 0.2308, respectively). An initial increase in TA was observed for all treatments from day 0 to day 6 after which a decline occurred. This is an indication of high metabolic ripening activities with the banana pulp, especially the conversion of starch to simple sugars. The conversion of starch or polysaccharides to simple sugars could result in the release of byproducts such as acidic metabolites. These metabolites have the potential to influence the TA of the banana pulp (Gupta et al., 2010). This finding is consistent with Mubarok et al. (2022) and Al-Dairi and Pathare (2024), who reported a similar trend in bananas during ripening where an initial increase in TA was observed till a peak before the commencement of a subsequent decline. The initial increase in TA increase was attributed to elevation in the organic acids present. Moreover, at peak TA (day 6), the control (0.53 ± 0.02) and MG (0.51 ± 0.01) treatments exhibited higher TA than the other treatments, which also aligns with observations by Watharkar et al. (2020) who observed a TA reduction after the ripening peak of banana during storage. These differences in the TA values during the banana

ripening also compared to the other studies were probably owing to the alterations in the metabolic activities induced by the formulations resulting in the release of different metabolites at varying concentrations. An increase in acidic metabolic will increase TA values. The TA values could also be modulated by interference in the metabolic processes by the antimicrobials in the formulated coat giving rise to lower titratable acidity, as titratable acidity and metabolic processes have an influenceable relationship. This is in collaboration with the report of Gupta et al. (2010) that titratable acidity and pH have an influenceable relationship or function with metabolic processes as well as the length of the processes.

For the observable TSS data, all treatments showed a significant rise in TSS from day 0 to day 6 ($p < 0.001$), except for the control, which plateaued after day 3. The increase in total soluble solids (TSS) over time reflects starch conversion to sugars during ripening. Reports have shown that during banana fruit maturation and ripening, gradual conversion of polysaccharide into simple sugars is expected and so higher TSS at the advanced stage of fruit ripening (Dadzie and Orchard, 1997; Lustriane et al., 2018). Post-day 6, all treatments exhibited significant decreases in TSS, except for ZnO + Ag, which only showed a notable reduction on day 12. This suggests that nanoparticle-based formulation treatments influence starch-to-sugar conversion through modulation of metabolic processes as well as effective in maintaining higher sugar content throughout the storage period, which aligns with Nxumalo et al. (2022), who observed higher TSS in ZnO-treated bananas by the end of storage. This could be ascribed to the inhibition or lowering of the metabolic processes (respiration and transpiration rate) of the banana fruit (Ahmad et al., 2001). Similarly, Shah and Hashmi (2020) reported that adding chitosan to *aloe vera* coating reduced weight loss, respiration rate, and ethylene production better than using chitosan only or control samples. Also, this treatment positively influences the fruit titratable acidity, total soluble solids, as well as fruit firmness, ascorbic acid, and color for longer shelf life. This can be attributed to the treatment potential to synergistically increases the phenolics of mango fruit, sustaining high ascorbic acid, and antioxidant activity during storage. This suggests coating might have enhanced the barricading potential of chitosan coating, thereby lowering the permeability of water and gaseous exchange (Mishra et al., 2010).

3.3.4 SEM: effect of NP on banana peel stomata

The potential effect of nanoparticle-based formulation on the banana peel was captured by SEM, and this is shown in Figure 8. As the banana ripens, brown spots, known as senescent spotting, appear. These spots are considered a type of programmed cell death (Anusornpornpong et al., 2024). These spots form in areas where stomata are present on the peel. Stomata serves as one of the primary pathways through which plants lose water (96–97%), making the maintenance of stomatal integrity crucial (Sampangi-Ramaiah et al., 2023). The stomata of the control showed little to no modulation of the structural integrity of the stomata (Figure 8A), indicating natural aging and senescence process without any treatment. Modulation of stomatal integrity and the quantity of guard cells correlate with postharvest fruit water loss (Zhang et al., 2021). This is also in agreement with results obtained in this study where the control had the highest weight loss. This can be ascribed to a lack of modulation in the stomatal cell to lower transpiration or water loss resulting from the absence of formulation treatment. When Moringa
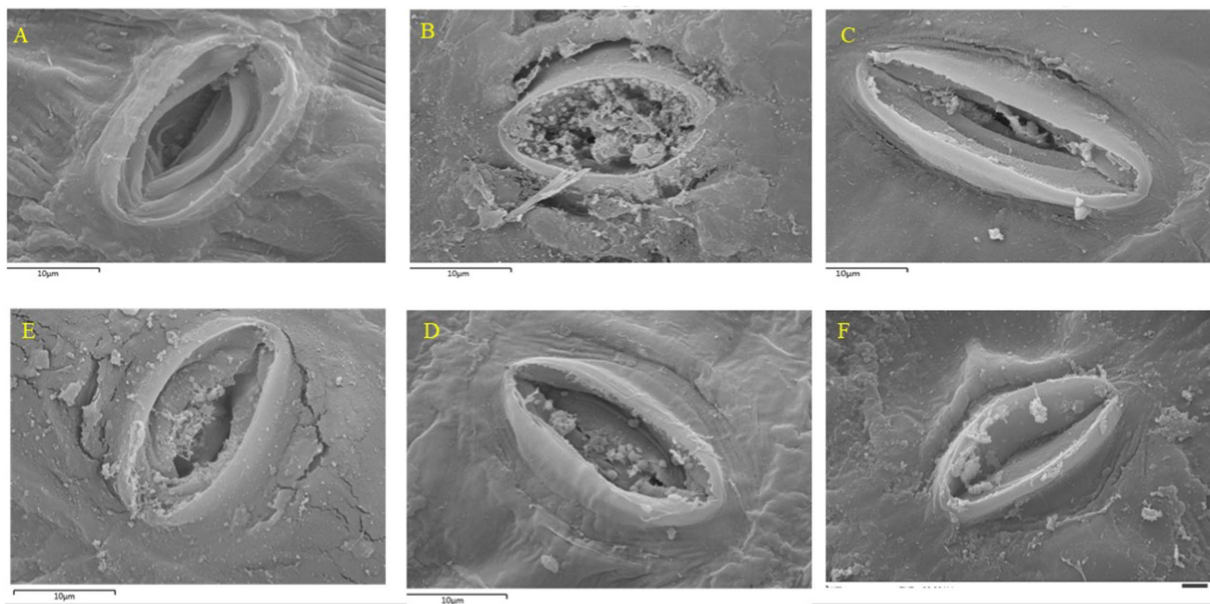
FIGURE 8
Effects of different nanoparticle treatments on stomatal behavior and preservation quality of banana peels over a 12-day storage period at 25°C. Stomatal observations were made on: **(A)** control (untreated) at day 12, **(B)** MG treatment at day 12, **(C)** MG + CMC + GLY treatment at day 12, **(D)** Ag$_2$O at day 12, **(E)** ZnO\at day 12, and **(F)** Ag$_2$O + ZnO at day 12.

was added, the stomata were partially clogged with Moringa debris, suggesting modulation from the MG treatment, some degradation over time (Figures 8B,C). This effect could be ascribed to the presence of CMC, GLY, and Moringa in the formulation which resulted in modulating the stomatal opening size, and visible guard cells compared to the control. These modulations or degradation (formulation with MG alone) could be due to the presence of high phytochemicals present in moringa formulation. In addition, Figures 8A,B (control and MG treatments) show wider stomatal openings than Figures 8D–F (nanoparticle treatments). Particularly, ZnO and Ag$_2$O + ZnO treatments exhibit more restricted stomatal openings, indicating reduced gas exchange. This suggests that these nanoparticle treatments may help limit water loss and slow down the ripening process by restricting gas exchange through the stomata. Nanoparticles at low concentrations in the formulations produced desirable effects. Nanoparticles at higher concentrations have been reported to have a toxic effect on biological cells. However, they are non-toxic or less harmful at low concentrations and rather exhibit biological catalytic potentials (Sanusi et al., 2019). Moreover, edible coatings fill fruit pores, mechanical cracks, and stomata, reducing gas exchange, regulating respiration, and lowering CO$_2$ production toward improve fruit quality matrices such as water loss, taste, peel coloration, and firmness (Luvielmo and Lamas, 2012; Navarro-Tarazaga et al., 2011; Kahramanoğlu et al., 2020). Oyom et al. (2022) demonstrated that 'early crisp,' an Asian pear, when coated with an edible coating made from sweet potato starch and infused with cumin essential oil, preserved stomatal integrity. Furthermore, the Ag$_2$O + ZnO formulation provided better protection against degradation by maintaining the integrity of the stomatal cells more effectively than single NP treatments. Previous studies (Avellan et al., 2021; Hu et al., 2020) suggest plant stomata as a potential route for NP entry. Additionally, as storage progresses and the fruit ripens, the stomatal

openings generally widen. Larger stomatal openings allow for increased gas exchange, which can enhance both transpiration and respiration rates. This might have accounted for more rapid water loss, leading to weight loss and dehydration in the control (Mukherjee et al., 2024).

3.3.4.1 Energy dispersed spectroscopy

The energy-dispersive X-ray spectroscopy (EDX) results shown in Figure 9 provide qualitative and quantitative information about the elemental composition of the samples. Each graph displays a spectrum with peaks corresponding to specific elements present in the samples. The control, MG, and MG + CMC + GLY samples contained carbon (C), oxygen (O), sodium (Na), silicon (Si), potassium (K), and calcium (Ca). When silver oxide (Ag$_2$O) was added, additional peaks for sulfur (S) and silver (Ag) were observed alongside the common elements. The addition of zinc oxide (ZnO) resulted in the appearance of zinc (Zn) along with the previously noted elements. When both Ag$_2$O and ZnO were introduced, the samples displayed peaks for both silver (Ag) and zinc (Zn), in addition to the common elements, confirming the integration of these compounds.

3.4 Principal component analysis biplot and hierarchal clustering heat map

The principal component analysis (PCA) was performed to reduce the dimensionality of the dataset and to identify the key variables influencing the different nanoparticle (NP) treatments. The first principal component (PC1) explains 63.03% of the variance in the data, indicating that more than half of the variability can be understood through this single component. The second principal component (PC2) explains an additional 19.40% of the variance.
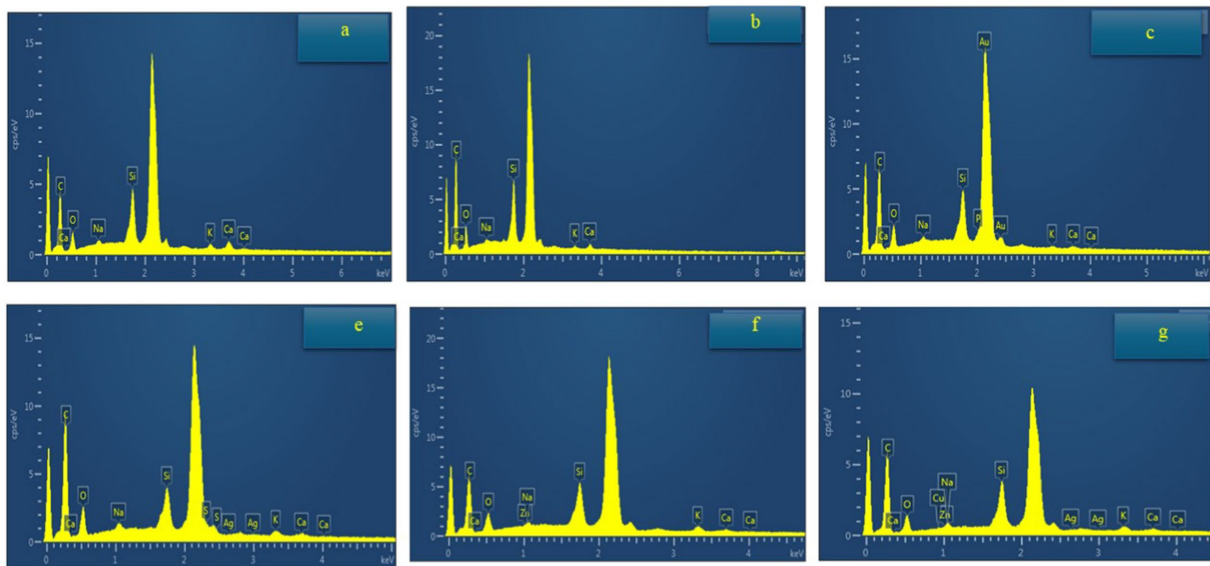
FIGURE 9
Energy-dispersive spectroscopy analysis of banana peel to determine elemental composition changes over a 12-day storage period at 25°C. Observations were made on: **(A)** Control (untreated) at day 12, **(B)** MG-treated peel at day 12, **(C)** MG + CMC + GLY-treated peel at day 12, **(E)** Ag_2O-treated peel at day 12, **(F)** ZnO-treated peel at day 12, and **(G)** Ag_2O + ZnO-treated peel at day 12.
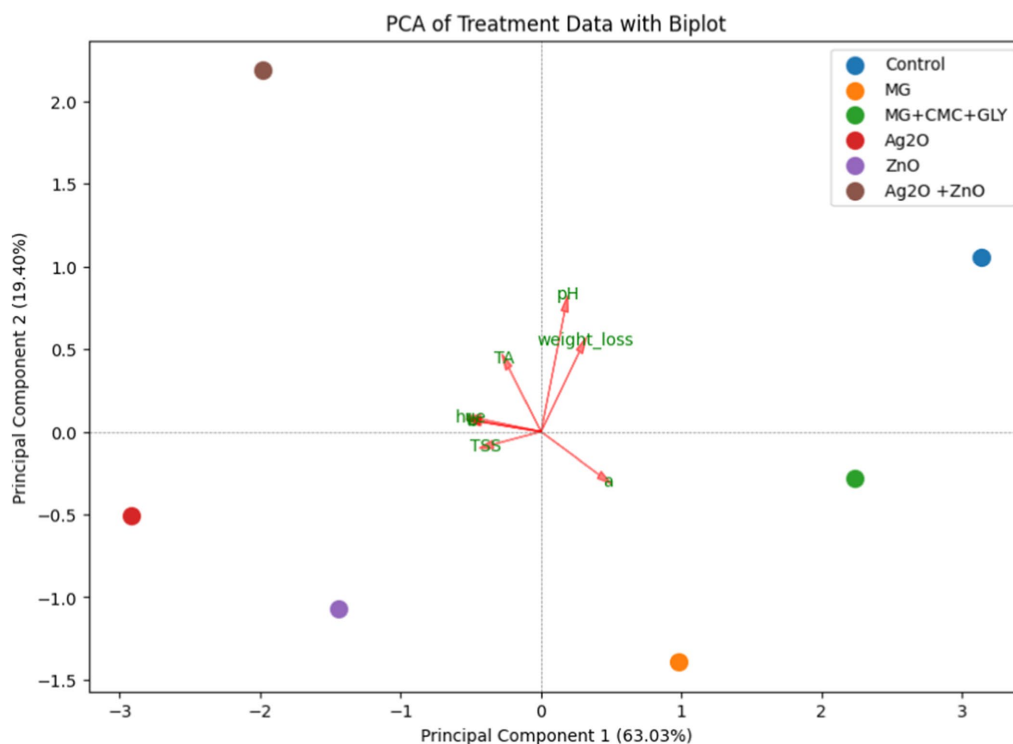
FIGURE 10
Principal component analysis (PCA) biplot of NP treatments and other characteristics {color (L, a, b, hue angle), weight loss, total soluble solids (TSS), pH, and titratable acidity (TA)}. Each point represents the treatment used, colored according to the type. The vectors indicate the contribution of each original variable (L*, a*, b*, hue, weight loss, pH, TA, and TSS) to the principal components. The length and direction of the vectors show the influence of the variables on the principal components. The longer the length the higher the significance of the contribution of the variable.
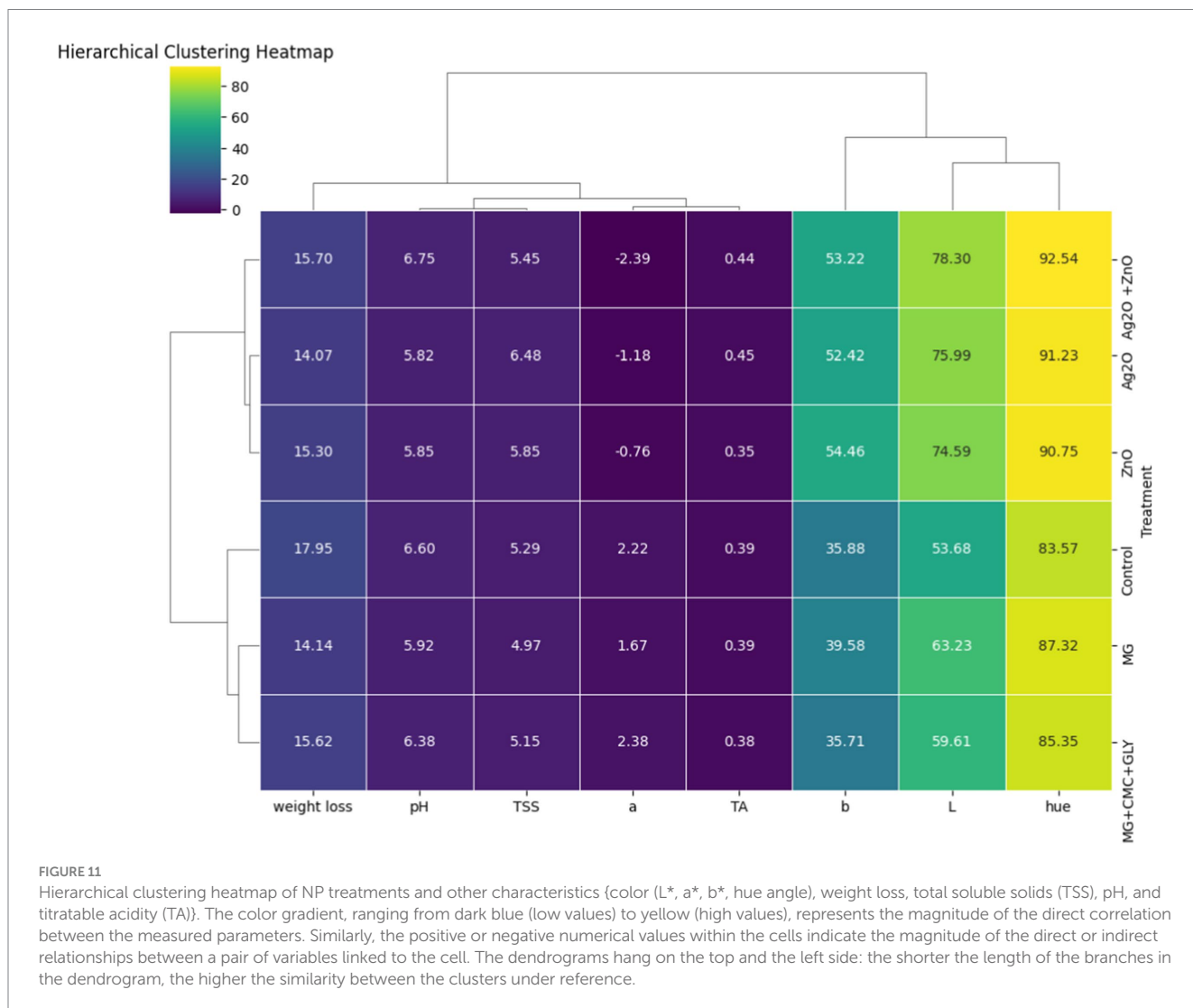
FIGURE 11
Hierarchical clustering heatmap of NP treatments and other characteristics {color (L*, a*, b*, hue angle), weight loss, total soluble solids (TSS), pH, and titratable acidity (TA)}. The color gradient, ranging from dark blue (low values) to yellow (high values), represents the magnitude of the direct correlation between the measured parameters. Similarly, the positive or negative numerical values within the cells indicate the magnitude of the direct or indirect relationships between a pair of variables linked to the cell. The dendrograms hang on the top and the left side: the shorter the length of the branches in the dendrogram, the higher the similarity between the clusters under reference.

TABLE 3 Weight of each variable in the principal components.

Variable	PC1	PC2
L*	−0.435212	0.061661
a*	0.414894	−0.259887
b*	−0.424032	0.060053
Hue	−0.432000	0.077438
Weight loss	0.273528	0.484910
pH	0.168167	0.727385
TA	−0.228030	0.385729
TSS	−0.341952	−0.077724

Together, PC1 and PC2 explain 82.43% of the total variability in the data. This high percentage of variance explained by PC1 and PC2 indicates that these components capture most of the important differences between treatments.

Table 3 displays the weight and direction of the contribution of the variables to the principal components visually elaborated by the PCA biplot (Figure 10). Each point in the biplot represents a different treatment (Control, MG, MG + CMC + GLY, Ag_2O, ZnO, and Ag_2O + ZnO), with the positions of the points indicating how the treatments relate to each other based on the principal components. In the biplot, the 'Control' treatment located at the far right along PC1 suggests that it is highly influenced by the variables that load heavily on this component (e.g., L*, a*, b*, and hue) and these are variables associated with color. In contrast, the Ag_2O and ZnO treatments are positioned on the left side of the biplot, indicating they are less influenced by the variables contributing to PC1. Particularly, the L*, b*, and hue are loading negatively on the PC1. This observation confirms the finding from the color assessment in Section 3.3 where at the end of the storage time, the highest L* and hue values were observed for the NP-treated bananas than the control.

Furthermore, in the biplot, the red arrows reveal the variables while depicting their respective impacts on the principal components. The direction and length of each arrow elucidate the magnitude of variable contributions: variables aligned with PC1 or PC2 indicate their predominant influence on these components. Thus, while 'a*' is prominently influencing PC1 positively, it influences PC2 negatively, consistent with its loadings (PC1: 0.414894, PC2: −0.259887; Table 1). This observation further confirms the findings on a* as earlier

discussed in Section 3.3., where its values were lesser for the NP-treated bananas than the control. It should be recalled that a higher a* value indicates a higher deviation from the green color toward red (decay).

Additionally, weight loss and pH show positive contributions to both PC1 and PC2, evident in their upward and rightward arrows (weight loss: PC1: 0.273528, PC2: 0.484910; pH: PC1: 0.168167, PC2: 0.727385). In contrast, variables, L, b, and hue exhibit negative contributions to PC1 (L: PC1: -0.435212, PC2: 0.061661; b: PC1: -0.424032, PC2: 0.060053; hue: PC1: -0.432000, PC2: 0.077438).

In the HCHM, bananas treated with ZnO and Ag_2O NPs show more positive influence on the variables 'L*', 'b*', and 'hue' than the non-treated (control) bananas (Figure 11). This is reflected in their higher numerical values: 'L*' (74.59), 'b*' (54.46), and 'hue' (90.75) for ZnO, and 'L*' (75.99), 'b*' (52.42), and 'hue' (91.23) for Ag_2O, than the control. This further confirms the earlier findings that the NPs particularly ZnO and Ag_2O positively influenced the color parameters in the NP-treated bananas. Aside from the correlation values, the similarity in the behavior of the ZnO and Ag_2O treatments is further evidenced by their proximity and clustering in the dendrogram, which indicates that these treatments have comparable effects on the measured parameters. This suggests that the combination of Ag_2O and ZnO may have a synergistic effect when compared to their individual applications. This observation aligns with the results from the decay incidence, color retention, and stomatal integrity analyses, which showed that the ZnO + Ag_2O was part of the treatments that had a positive impact on the color and structural integrity of the bananas. These findings further confirm that nanoparticles offer enhanced protection against decay.

4 Conclusion

This study demonstrated that ZnO and Ag_2O nanoparticles, both individually and as a composite, effectively enhanced the postharvest quality of 'Cavendish' bananas. By the end of the storage period, bananas treated with nanoparticles retained better color (L*, b*, a*, and h° values). In addition, the fruits treated with ZnO + Ag_2O nanoparticles demonstrated a significantly lower decay incidence of 44.44% than the control (100%). Additionally, PCA and HCHM analyses confirmed that ZnO and Ag_2O coatings positively affected key quality parameters such as weight loss, total acidity, pH, and total soluble solids, with the ZnO + Ag_2O combination proving to be the most effective at preserving overall fruit quality. Moreover, this report highlights the potential of nanoparticle-enriched edible coatings, especially the ZnO + Ag_2O composite, in extending the shelf life and marketability of bananas. While further research is necessary to evaluate the long-term safety of using nanoparticles in food preservation, these findings could significantly improve banana storage and transportation practices, helping reduce postharvest losses in the industry.

Data availability statement

The raw data supporting the conclusions of this article will be made available by the authors, without undue reservation.

Author contributions

NA: Conceptualization, Data curation, Formal analysis, Investigation, Methodology, Software, Visualization, Writing – original draft, Writing – review & editing. IS: Conceptualization, Methodology, Visualization, Writing – review & editing, Formal analysis, Investigation, Project administration, Writing – original draft. GA: Conceptualization, Methodology, Visualization, Writing – review & editing, Formal analysis, Investigation, Writing – original draft. AM: Writing – review & editing, Project administration, Resources, Supervision. ST: Conceptualization, Supervision, Writing – review & editing, Project administration, Resources.

Conflict of interest

The authors declare that the research was conducted in the absence of any commercial or financial relationships that could be construed as a potential conflict of interest.

Publisher's note

All claims expressed in this article are solely those of the authors and do not necessarily represent those of their affiliated organizations, or those of the publisher, the editors and the reviewers. Any product that may be evaluated in this article, or claim that may be made by its manufacturer, is not guaranteed or endorsed by the publisher.

References

Acevedo-Fani, A., Soliva-Fortuny, R., and Martín-Belloso, O. (2017). Nanoemulsions as edible coatings. *Curr. Opin. Food Sci.* 15, 43–49. doi: 10.1016/j.cofs.2017.06.002

Ahmad, S., Thompson, A. K., Hafiz, I. A., and Asi, A. A. (2001). Effect of temperature on the ripening and quality of banana fruit. *Int. J. Agric. Biol.* 3, 224–227.

Al-Dairi, M., and Pathare, P. B. (2024). Evaluation of physio-chemical characteristics of 'Fard' banana using computer vision system. *J. Agric. Food Res.* 15:101057. doi: 10.1016/j.jafr.2024.101057

Al-Dairi, M., Pathare, P. B., Al-Yahyai, R., Jayasuriya, H., and Al-Attabi, Z. (2024). Evaluation of chemical quality attributes in bruised bananas during storage. *LWT* 197:115904. doi: 10.1016/j.lwt.2024.115904

Anusornpornpong, P., Chuenwarin, P., Sonong, A., Srihiran, Y., Buensanteai, K., and Imsabai, W. (2024). Type of stomata and peel structure associated with programmed cell death of senescent spotting in banana. *Sci. Hortic.* 332:113231. doi: 10.1016/j.scienta.2024.113231

Araujo, E. A., Andrade, N. J., da Silva, L. H. M., Bernardes, P. C., Teixeira, A. V. D. C., de Sa, J. P. N., et al. (2012). Antimicrobial effects of silver nanoparticles against bacterial cells adhered to stainless steel surfaces. *J. Food Prot.* 75, 701–705. doi: 10.4315/0362-028X.JFP-11-276

Atta-Aly, M. A. (1992). Effect of high temperature on ethylene bio synthesis by tomato fruit. *Postharvest Biol. Technol.* 2, 19–24. doi: 10.1016/0925-5214(92)90023-I

Avellan, A., Yun, J., Morais, B. P., Clement, E. T., Rodrigues, S. M., and Lowry, G. V. (2021). Critical review: role of inorganic nanoparticle properties on their foliar uptake and in planta translocation. *Environ. Sci. Technol.* 55, 13417–13431. doi: 10.1021/acs.est.1c00178

Baldwin, E. A., Burns, J. K., and Kazokas, W. (1991). Effect of two edible coatings with different permeability characteristics on mango (Mangifera indica L.) ripening during storage. *Post Harvest Biol. Tech.* 17, 215–226. doi: 10.1016/S0925-5214(99)00053-8

Becerril-Sánchez, A. L., Quintero-Salazar, B., Dublán-García, O., and Escalona-Buendía, H. B. (2021). Phenolic compounds in honey and their relationship with antioxidant activity, botanical origin, and color. *Antioxidants* 10:1700. doi: 10.3390/antiox10111700

Belay, Z. A., Caleb, O. J., and Opara, U. L. (2019). Influence of initial gas modification on physicochemical quality attributes and molecular changes in fresh and fresh-cut fruit during modified atmosphere packaging. *Food Packag. Shelf Life* 21:100359. doi: 10.1016/j.fpsl.2019.100359

Chandirika, J. U., Selvi, S. T., and Annadurai, G. (2018). Synthesis and characterization of silver nanoparticle using Melia azedarach for vegetable coating and antibacterial activity. *J. Innov. Pharm. Biol. Sci.* 5, 38–42.

Chawla, R., Sivakumar, S., and Kaur, H. (2021). Antimicrobial edible films in food packaging: current scenario and recent nanotechnological advancements-a review. *Carbohyd. Poly. Tech. Appl.* 2:100024. doi: 10.1016/j.carpta.2020.100024

Coimbra, P., Marona, B., Henriques, M. H., Campos, L., Gomes, D. M., Vitorino, C., et al. (2023). Edible films based on potato and quince peels with potential for the preservation of cured cheese. *Food Packag. Shelf Life* 40:101176. doi: 10.1016/j.fpsl.2023.101176

Dadzie, B. K., and Orchard, J. E. (1997). Routine postharvest screening of banana/plantain hybrids criteria and methods, international network for banana and plantain (Inibap). Rome, Italy: Technical Guide lines.

Dale, J., Paul, J. Y., Dugdale, B., and Harding, R. (2017). Modifying bananas: from transgenics to organics? *Sustain. For.* 9:333. doi: 10.3390/su9030333

Dhall, R. K. (2013). Advances in edible coatings for fresh fruits and vegetables: a review. *Crit. Rev. Food Sci. Nutr.* 53, 435–450. doi: 10.1080/10408398.2010.541568

Dwivany, F. M., Aprilyandi, A. N., Suendo, V., and Sukriandi, N. (2020). Carrageenan edible coating application prolongs Cavendish banana shelf life. *Int. J. Food Sci.* 2020, 1–11. doi: 10.1155/2020/8861610

Esparza-González, S. C., Sánchez-Valdés, S., Ramírez-Barrón, S. N., Loera-Arias, M. J., Bernal, J., Meléndez-Ortiz, H. I., et al. (2016). Effects of different surface modifying agents on the cytotoxic and antimicrobial properties of ZnO nanoparticles. *Toxicol. in Vitro* 37, 134–141. doi: 10.1016/j.tiv.2016.09.020

Fukano, Y., and Tachiki, Y. (2021). Evolutionary ecology of climacteric and non-climacteric fruits. *Biol. Lett.* 17:20210352. doi: 10.1098/rsbl.2021.0352

Gad, M. M., and Zagzog, O. A. (2017). Mixing xanthan gum and chitosan nano particles to form new coating for maintaining storage life and quality of elmamoura guava fruits. *Int. J. Curr. Microbiol. App. Sci.* 6, 1582–1591. doi: 10.20546/ijcmas.2017.611.190

Geng, J., O'Dell, J., Stark, N., Kitin, P., Zhang, X., and Zhu, J. Y. (2024). Microfibrillated cellulose (MFC) barrier coating for extending banana shelf life. *Food Hydrocoll.* 150:109671. doi: 10.1016/j.foodhyd.2023.109671

Giovannoni, J., Nguyen, C., Ampofo, B., Zhong, S., and Fei, Z. (2017). The epigenome and transcriptional dynamics of fruit ripening. *Annu. Rev. Plant Biol.* 68, 61–84. doi: 10.1146/annurev-arplant-042916-040906

Gularte, P. S., Steffens, C. A., Cerezer, B., Miqueloto, T., da Silva, J. C., Heinzen, A. S., et al. (2022). Use of nitric oxide for ripening delay and oxidative stress reduction in Cavendish banana stored in a controlled atmosphere. *J. Food Process. Preserv.* 46:e16926. doi: 10.1111/jfpp.16926

Gupta, M., Abu-Ghannam, N., and Gallaghar, E. (2010). Barley for brewing: Characteristic changes during malting, brewing and applications of its by-products. *Compr. Rev. Food Sci. Food Saf.* 9, 318–328. doi: 10.1111/j.1541-4337.2010.00112.x

Hasan, M. U., Riaz, R., Malik, A. U., Khan, A. S., Anwar, R., Rehman, R. N. U., et al. (2021). Potential of Aloe vera gel coating for storage life extension and quality conservation of fruits and vegetables: An overview. *J. Food Biochem.* 45:e13640. doi: 10.1111/jfbc.13640

Hossain, M. S., and Iqbal, A. (2016). Effect of shrimp chitosan coating on postharvest quality of banana (Musa sapientum L.) fruits. *Int. Food Res. J.* 23, 277–283.

Hu, P., An, J., Faulkner, M. M., Wu, H., Li, Z., Tian, X., et al. (2020). Nanoparticle charge and size control foliar delivery efficiency to plant cells and organelles. *ACS Nano* 14, 7970–7986. doi: 10.1021/acsnano.9b09178

Hudina, M., Stampar, F., Orazem, P., Petkovsek, M. M., and Veberic, R. (2012). Phenolic compounds profile, carbohydrates and external fruit quality of the

'Concorde'pear (Pyrus communis L.) after bagging. *Can. J. Plant Sci.* 92, 67–75. doi: 10.4141/cjps2011-095

Joshy, K. S., Jose, J., Li, T., Thomas, M., Shankregowda, A. M., Sreekumaran, S., et al. (2020). Application of novel zinc oxide reinforced xanthan gum hybrid system for edible coatings. *Int. J. Biol. Macromol.* 151, 806–813. doi: 10.1016/j.ijbiomac.2020.02.085

Kahramanoğlu, İ., Chen, C., Gan, Z., Chen, J., and Wan, C. (2020). The effects of edible coatings on the postharvest quality of citrus fruits as affected by granulation. *J. Food Qual.* 2020, 1–8. doi: 10.1155/2020/8819233

Kapoor, L., Simkin, A. J., George Priya Doss, C., and Siva, R. (2022). Fruit ripening: dynamics and integrated analysis of carotenoids and anthocyanins. *BMC Plant Biol.* 22:27. doi: 10.1186/s12870-021-03411-w

Karoney, E. M., Molelekoa, T., Bill, M., Siyoum, N., and Korsten, L. (2024). Global research network analysis of fresh produce postharvest technology: innovative trends for loss reduction. *Postharvest Biol. Technol.* 208:112642. doi: 10.1016/j.postharvbio.2023.112642

Ke, D., and Kader, A. (1989). "Tolerance and responses of fresh fruits to oxygen levels at or below 1%," in *Proceedings of the 5th International Controlled Atmosphere Research Conference*. 2, 209–216, Wenatchee, Washington.

Khalid, M. A., Niaz, B., Saeed, F., Afzaal, M., Islam, F., Hussain, M., et al. (2022). Edible coatings for enhancing safety and quality attributes of fresh produce: a comprehensive review. *Int. J. Food Prop.* 25, 1817–1847. doi: 10.1080/10942912.2022.2107005

Khaliq, G., Abbas, H. T., Ali, I., and Waseem, M. (2019). Aloe vera gel enriched with garlic essential oil effectively controls anthracnose disease and maintains postharvest quality of banana fruit during storage. *Hortic. Environ. Biotechnol.* 60, 659–669. doi: 10.1007/s13580-019-00159-z

Kim, J., Choi, J. Y., Kim, J., and Moon, K. D. (2022). Effect of edible coating with Morus alba root extract and carboxymethyl cellulose for enhancing the quality and preventing the browning of banana (Musa acuminata Cavendish) during storage. *Food Packag. Shelf Life* 31:100809. doi: 10.1016/j.fpsl.2022.100809

Kumar, H., Manisha, S. P., and Sangwan, P. (2013). Synthesis and Characterization of MnO2 Nanoparticles using Co-precipitation Technique. *Int. J. Chem. Chem. Eng.* 3, 155–160.

Lang, C., Mission, E. G., Fuaad, A. A. H. A., and Shaalan, M. (2021). Nanoparticle tools to improve and advance precision practices in the Agrifoods sector towards sustainability-a review. *J. Clean. Prod.* 293:126063. doi: 10.1016/j.jclepro.2021.126063

Li, S., Chen, K., and Grierson, D. (2021). Molecular and hormonal mechanisms regulating fleshy fruit ripening. *Cells* 10:1136. doi: 10.3390/cells10051136

Li, X., Li, W., Jiang, Y., Ding, Y., Yun, J., Tang, Y., et al. (2019). Effect of nano-ZnO-coated active packaging on quality of fresh-cut 'Fuji' apple. *Int. J. Food Sci. Technol.* 54, 2400–2409.

Li, S., Wu, P., Yu, X., Cao, J., Chen, X., Gao, L., et al. (2022). Contrasting roles of ethylene response factors in pathogen response and ripening in fleshy fruit. *Cells* 11:2484. doi: 10.3390/cells11162484

Lustriane, C., Dwivany, F. M., Suendo, V., and Reza, M. (2018). Effect of chitosan and chitosan-nanoparticles on post harvest quality of banana fruits. *J. Plant Biotechnol.* 45, 36–44. doi: 10.5010/JPB.2018.45.1.036

Luvielmo, M. M., and Lamas, S. V. (2012). Edible coatings for fruits. *Estudos Tecnológicos em Engenharia* 8, 8–15. doi: 10.4013/ete.2012.81.02

Malekshahi, G., and ValizadehKaji, B. (2021). Effects of postharvest edible coatings to maintain qualitative properties and to extend shelf-life of pomegranate (*Punica granatum* L). *Int. J. Hortic. Sci. Tech.* 8, 67–80. doi: 10.22059/ijhst.2020.296297.337

Maoka, T. (2020). Carotenoids as natural functional pigments. *J. Nat. Med.* 74, 1–16. doi: 10.1007/s11418-019-01364-x

Maqbool, M., Ali, A., Alderson, P. G., Zahid, N., and Siddiqui, Y. (2011). Effect of a novel edible composite coating based on gum arabic and chitosan on biochemical and physiological responses of banana fruits during cold storage. *J. Agric. Food Chem.* 59, 5474–5482. doi: 10.1021/jf200623m

Matas, A. J., Gapper, N. E., Chung, M. Y., Giovannoni, J. J., and Rose, J. K. (2009). Biology and genetic engineering of fruit maturation for enhanced quality and shelf-life. *Curr. Opin. Biotechnol.* 20, 197–203. doi: 10.1016/j.copbio.2009.02.015

Meindrawan, B., Suyatma, N. E., Wardana, A. A., and Pamela, V. Y. (2018). Nanocomposite coating based on carrageenan and ZnO nanoparticles to maintain the storage quality of mango. *Food Packag. Shelf Life* 18, 140–146. doi: 10.1016/j.fpsl.2018.10.006

Mishra, B., Khatkar, B. S., Garg, M. K., and Wilson, L. A. (2010). Permeability of edible coatings. *J. Food Sci. Technol.* 47, 109–113. doi: 10.1007/s13197-010-0003-7

Mubarok, S., Maulida Rahman, I., Nuraniya Kamaluddin, N., and Solihin, E. (2022). Impact of 1-Methylcyclopropene combined with chitosan on postharvest quality of tropical banana 'lady finger'. *Int. J. Food Prop.* 25, 1171–1185. doi: 10.1080/10942912.2022.2074028

Mukherjee, S., Paul, S., and Mitra, A. (2024). Unravelling physiological and histochemical changes in two popular dessert and cooking bananas of India during fruit ripening. *Sci. Hortic.* 336:113409. doi: 10.1016/j.scienta.2024.113409

Navarro-Tarazaga, M. L., Massa, A., and Pérez-Gago, M. B. (2011). Effect of beeswax content on hydroxypropyl methylcellulose-based edible film properties and postharvest

quality of coated plums (Cv. Angeleno). LWT-food. *Sci. Technol.* 44, 2328–2334. doi: 10.1016/j.lwt.2011.03.011

Nde, S. C., Felicite, O. M., Aruwajoye, G. S., and Palamuleni, L. G. (2024). A meta-analysis and experimental survey of heavy metals pollution in agricultural soils. *J. Trace Elements Min.* 9:100180. doi: 10.1016/j.jtemin.2024.100180

Nuamduang, P., Winotapun, C., Harnkarnsujarit, N., Sungdech, P., Issaraseree, Y., and Leelaphiwat, P. (2024). Regulating gas transmission rates in microperforated polybutylene succinate films for modified atmosphere packaging of bananas. *Food Packag. Shelf Life* 45:101347. doi: 10.1016/j.fpsl.2024.101347

Nxumalo, K. A., Fawole, O. A., and Oluwafemi, O. S. (2022). Evaluating the efficacy of gum arabic-zinc oxide nanoparticles composite coating on shelf-life extension of mandarins (cv. kinnow). *Front. Plant Sci.* 13:953861. doi: 10.3389/fpls.2022.953861

Odetayo, T., Sithole, L., Shezi, S., Nomngongo, P., Tesfay, S., and Ngobese, N. Z. (2022). Effect of nanoparticle-enriched coatings on the shelf life of Cavendish bananas. *Sci. Hortic.* 304:111312. doi: 10.1016/j.scienta.2022.111312

Olunusi, S. O., Ramli, N. H., Fatmawati, A., Ismail, A. F., and Okwuwa, C. C. (2024). Revolutionizing tropical fruits preservation: Emerging edible coating technologies. *Int. J. Biol. Macromol.* 264:130682. doi: 10.1016/j.ijbiomac.2024.130682

Ortiz-Duarte, G., Pérez-Cabrera, L. E., Artés-Hernández, F., and Martínez-Hernández, G. B. (2019). Ag-chitosan nanocomposites in edible coatings affect the quality of fresh-cut melon. *Postharvest Biol. Technol.* 147, 174–184. doi: 10.1016/j.postharvbio.2018.09.021

Othman, S. H., Abdullah, N. A., Nordin, N., Shah, N. N. A. K., Nor, M. Z. M., and Yunos, K. F. M. (2021). Shelf life extension of Saba banana: effect of preparation, vacuum packaging, and storage temperature. *Food Packag. Shelf Life* 28:100667. doi: 10.1016/j.fpsl.2021.100667

Oyom, W., Hengping, X., Liu, Z., Long, H., Li, Y., Zhang, Z., et al. (2022). Effects of modified sweet potato starch edible coating incorporated with cumin essential oil on storage quality of 'early crisp'. *LWT* 153:112475. doi: 10.1016/j.lwt.2021.112475

Park, H. J., Weller, C. L., Vergano, P. J., and Testin, R. F. (1993). Perme ability and mechanical properties of cellulose-based edible films. *J. Food Sci.* 58, 1361–1364. doi: 10.1111/j.1365-2621.1993.tb06183.x

Paulo, A. F. S., Baú, T. R., Ida, E. I., and Shirai, M. A. (2021). Edible coatings and films with incorporation of prebiotics—a review. *Food Res. Int.* 148:110629. doi: 10.1016/j.foodres.2021.110629

Pereira, L., Santo Domingo, M., Argyris, J., Mayobre, C., Valverde, L., Martín-Hernández, A. M., et al. (2021). A novel introgression line collection to unravel the genetics of climacteric ripening and fruit quality in melon. *Sci. Rep.* 11:11364. doi: 10.1038/s41598-021-90783-6

Ponce, C., Kuhn, N., Arellano, M., Time, A., Multari, S., Martens, S., et al. (2021). Differential phenolic compounds and hormone accumulation patterns between early- and mid-maturing sweet cherry (Prunus avium L.) cultivars during fruit development and ripening. *J. Agric. Food Chem.* 69, 8850–8860. doi: 10.1021/acs.jafc.1c01140

Rahman, A. N. F., Muhammad, V. C., and Bastian, F. (2021). Effect of storage temperature on the quality of kepok banana (Musa paradisiaca formatypica). *Canrea J.: Food Technol. Nutr. Culin. J.* 4, 17–47. doi: 10.20956/canrea.v4i1.338

Ribeiro, S. R., Garcia, M. V., Copetti, M. V., Brackmann, A., Both, V., and Wagner, R. (2021). Effect of controlled atmosphere, vacuum packaging and different temperatures on the growth of spoilage fungi in shelled pecan nuts during storage. *Food Control* 128:108173. doi: 10.1016/j.foodcont.2021.108173

Romero, J., Albertos, I., Díez-Méndez, A., and Poveda, J. (2022). Control of postharvest diseases in berries through edible coatings and bacterial probiotics. *Sci. Hortic.* 304:111326. doi: 10.1016/j.scienta.2022.111326

Saleem, M. S., Anjum, M. A., Naz, S., Ali, S., Hussain, S., Azam, M., et al. (2021). Incorporation of ascorbic acid in chitosan-based edible coating improves postharvest quality and storability of strawberry fruits. *Int. J. Biol. Macromol.* 189, 160–169. doi: 10.1016/j.ijbiomac.2021.08.051

Sampangi-Ramaiah, M. H., Shivashankara, K. S., Rekha, A., Laxman, R. H., Dayanandhi, E., and Ravishankar, K. V. (2023). High-density GBS-based genetic linkage map construction and QTL identification associated with leaf cuticular wax, adaxial stomatal density and leaf water retention capacity in banana. *Sci. Hortic.* 321:112205. doi: 10.1016/j.scienta.2023.112205

Sanusi, I., Aruwajoye, G., Revaprasadu, N., Sewsynker-Sukai, Y., Meyer, E. L., and Gueguim-Kana, E. B. (2022). A novel autoclave-assisted nanoparticle pre-treatment for improved sugar recovery from potato peel waste: process optimisation, nanoparticle recyclability and bioethanol production. *Biomass Convers. Biorefinery* 14, 13941–13953. doi: 10.1007/s13399-022-03574-y

Sanusi, I. A., Faloye, F. D., and Gueguim, K. E. (2019). Impact of various metallic oxide nanoparticles on ethanol production by Saccharomyces cerevisiae BY4743: screening, kinetic study and validation on potato waste. *Catal. Lett.* 149, 2015–2031. doi: 10.1007/s10562-019-02796-6

Sanusi, A. I., Suinyuy, T. N., Lateef, A., and Gueguim Kana, E. A. (2020). Effect of nickel oxide nanoparticles on bioethanol production: Process optimization, kinetic and metabolic studies. *Process Biochem.* 92, 386–400. doi: 10.1016/j.procbio.2020.01.029

Severino, R., Vu, K. D., Donsì, F., Salmieri, S., Ferrari, G., and Lacroix, M. (2014). Antibacterial and physical effects of modified chitosan based-coating containing nanoemulsion of mandarin essential oil and three non-thermal treatments against Listeria innocua in green beans. *Int. J. Food Microbiol.* 191, 82–88. doi: 10.1016/j.ijfoodmicro.2014.09.007

Shah, S., and Hashmi, M. S. (2020). Chitosan–aloe vera gel coating delays postharvest decay of mango fruit. *Hortic. Environ. Biotechnol.* 61, 279–289. doi: 10.1007/s13580-019-00224-7

Shi, Y., Li, B. J., Su, G., Zhang, M., Grierson, D., and Chen, K. S. (2022). Transcriptional regulation of fleshy fruit texture. *J. Integr. Plant Biol.* 64, 1649–1672. doi: 10.1111/jipb.13316

Shinga, M. H., and Fawole, O. A. (2023). Opuntia ficus indica mucilage coatings regulate cell wall softening enzymes and delay the ripening of banana fruit stored at retail conditions. *Int. J. Biol. Macromol.* 245:125550. doi: 10.1016/j.ijbiomac.2023.125550

Singh, V., Hedayetullah, M., Zaman, P., and Meher, J. (2014). Postharvest technology of fruits and vegetables: An overview. *J. Postharvest Tech.* 2, 124–135.

Soradech, S., Nunthanid, J., Limmatvapirat, S., and Luangtana-anan, M. (2017). Utilization of shellac and gelatin composite film for coating to extend the shelf life of banana. *Food Control* 73, 1310–1317. doi: 10.1016/j.foodcont.2016.10.059

Sorrentino, A., Gorrasi, G., and Vittoria, V. (2007). Potential perspectives of bio-nanocomposites for food packaging applications. *Trends Food Sci. Technol.* 18, 84–95. doi: 10.1016/j.tifs.2006.09.004

Sruthi, P. S., Balasubramanian, S., Kumar, P. S., Kapoor, A., Ponnuchamy, M., Jacob, M. M., et al. (2021). Eco-friendly pH detecting paper-based analytical device: towards process intensification. *Anal. Chim. Acta* 1182:338953. doi: 10.1016/j.aca.2021.338953

Thewes, F. R., Both, V., Brackmann, A., Thewes, F. R., Soldateli, F. J., Berghetti, M. R. P., et al. (2022). Dynamic and static drying temperatures for 'Barton'pecans: Impacts on the volatile compounds profile and kernel color. *LWT* 161:113393. doi: 10.1016/j.lwt.2022.113393

Vilaplana, R., Guerrero, K., Guevara, J., and Valencia-Chamorro, S. (2020). Chitosan coatings to control soft mold on fresh blackberries (Rubus glaucus Benth.) during postharvest period. *Sci. Hortic.* 262:109049. doi: 10.1016/j.scienta.2019.109049

Vizhi, D. K., Supraja, N., Devipriya, A., Tollamadugu, N. V. K. V. P., and Babujanarthana, R. (2016). Evaluation of antibacterial activity and cytotoxic effects of green AgNPs against Breast Cancer Cells (MCF 7). *Adv. Nano Res.* 4, 129–143. doi: 10.12989/anr.2016.4.2.129

Wahab, A., Rahim, A. A., Hassan, S., Egbuna, C., Manzoor, M. F., Okere, K. J., et al. (2021). "Chapter 10 - Application of nanotechnology in the packaging of edible materials," in *Preparation of phytopharmaceuticals for the management of disorders.* Academic Press, 215–225.

Wall, M. M., and Gentry, T. S. (2007). Carbohydrate composition and color development during drying and roasting of macadamia nuts (Macadamia integrifolia). *LWT Food Sci. Tech.* 40, 587–593. doi: 10.1016/j.lwt.2006.03.015

Watharkar, R. B., Pu, Y., Ismail, B. B., Srivastava, B., Srivastav, P. P., and Liu, D. (2020). Change in physicochemical characteristics and volatile compounds during different stage of banana (Musa nana Lour vs. dwarf Cavendish) ripening. *J. Food Meas. Charact.* 14, 2040–2050. doi: 10.1007/s11694-020-00450-z

Wilson, M. D., Stanley, R. A., Eyles, A., and Ross, T. (2019). Innovative processes and technologies for modified atmosphere packaging of fresh and fresh-cut fruits and vegetables. *Crit. Rev. Food Sci. Nutr.* 59, 411–422. doi: 10.1080/10408398.2017.1375892

Xiang, W., Wang, H. W., Tian, Y., and Sun, D. W. (2021). Effects of salicylic acid combined with gas atmospheric control on postharvest quality and storage stability of wolfberries: quality attributes and interaction evaluation. *J. Food Process Eng.* 44:e13764. doi: 10.1111/jfpe.13764

Yousuf, B., Qadri, O. S., and Srivastava, A. K. (2018). Recent developments in shelf-life extension of fresh-cut fruits and vegetables by application of different edible coatings: a review. *LWT* 89, 198–209. doi: 10.1016/j.lwt.2017.10.051

Zhang, Y. L., Cui, Q. L., Wang, Y., Shi, F., Fan, H., Zhang, Y. Q., et al. (2021). Effect of edible carboxymethyl chitosan-gelatin based coating on the quality and nutritional properties of different sweet cherry cultivars during postharvest storage. *Coatings* 11:396. doi: 10.3390/coatings11040396

Zhang, H., Mahunu, G. K., Castoria, R., Apaliya, M. T., and Yang, Q. (2017). Augmentation of biocontrol agents with physical methods against postharvest diseases of fruits and vegetables. *Trends Food Sci. Technol.* 69, 36–45. doi: 10.1016/j.tifs.2017.08.020

Zhou, X., Hu, W., Li, J., Iqbal, A., Murtaza, A., Xu, X., et al. (2022). High-pressure carbon dioxide treatment and vacuum packaging alleviate the yellowing of peeled Chinese water chestnut (Eleocharis tuberosa). *Food Packag. Shelf Life* 34:100927. doi: 10.1016/j.fpsl.2022.100927